CHALMERS
UNIVERSITY OF TECHNOLOGY

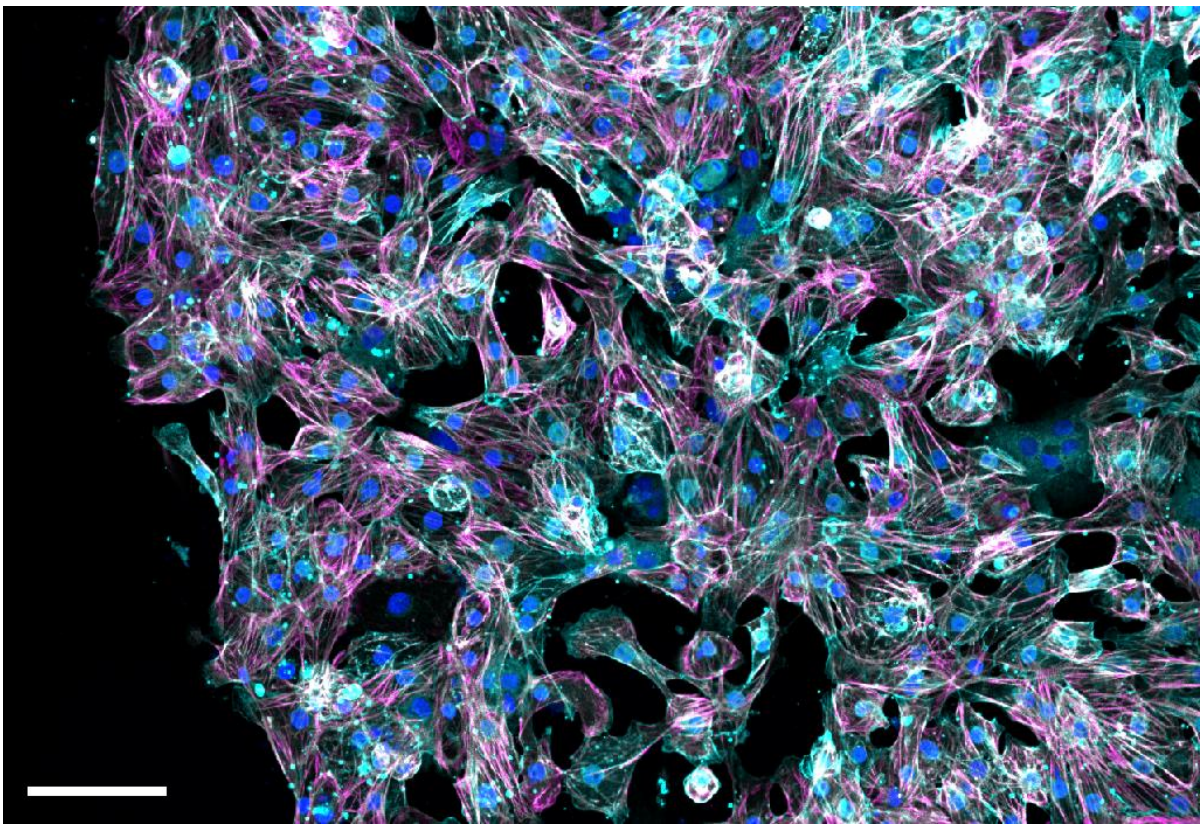

Development and evaluation of an *in vitro* cardiovascular model for determining impact of genetic variability in calcium handling on drug-induced cardiotoxicity

Master's thesis in Biotechnology

MICHELLE KHA

Department of Physics
Division of Biological Physics
CHALMERS UNIVERSITY OF TECHNOLOGY
Gothenburg, Sweden 2019

Development and evaluation of an *in vitro* cardiovascular model for determining impact of genetic variability in calcium handling on drug-induced cardiotoxicity

MICHELLE KHA

Department of Physics
Division of Biological Physics
CHALMERS UNIVERSITY OF TECHNOLOGY
Gothenburg, Sweden 2019

Development and evaluation of an *in vitro* cardiovascular model for determining impact of genetic variability in calcium handling on drug-induced cardiotoxicity
MICHELLE KHA

Supervisor: Linda Starnes, Drug Safety and Metabolism, Innovative Medicines and Early Development, AstraZeneca

Examiner: Julie Gold, Division of Biological Physics, Department of Physics, Chalmers University of Technology

Department of Physics
Division of Biological Physics
Chalmers University of Technology
SE-412 96 Gothenburg
Sweden
Telephone + 46 (0)31-772 1000

Cover: Immunocytochemistry image of human induced pluripotent stem cell-derived cardiomyocytes, stained with cardiac troponin T in magenta and alpha-actinin in cyan, obtained by confocal microscope. Scalebar=100 µm.

Printed by Department of Physics
Gothenburg, Sweden 2019

Development and evaluation of an *in vitro* cardiovascular model for determining impact of genetic variability in calcium handling on drug-induced cardiotoxicity

MICHELLE KHA
Department of Physics
Division of Biological Physics
Chalmers University of Technology

Abstract

Cardiotoxicity is evaluated throughout the process of drug discovery and development and is a leading cause of drug attrition during clinical trials. One of the major challenges includes the understanding of differential pharmacology responses in healthy and disease states. This can be improved by the development of human *in vitro* models and consideration of genetic variability in patients. In this thesis, a human induced pluripotent stem cell (hiPSC) line was developed with a heterozygous single nucleotide polymorphism (SNP) rs3766871 (G1886S) within a calcium handling gene, *RYR2*. This SNP is the second most common heterozygous SNP within *RYR2* and has been associated with cardiac diseases. The SNP line was obtained by reverse transfection of hiPSCs using CRISPR/Cas9 and was validated by Sanger sequencing. Furthermore, an existing hiPSC line with a heterozygous knock-out within *RYR2* was evaluated in this thesis. The heterozygous knock-out hiPSC line mimics the partial reduction of RYR2 expression observed in aging and heart disease. This line was differentiated into cardiomyocytes and characterized by FACS, ICC and Western blotting. In addition, impedance-based measurements were conducted as a surrogate of contractility to obtain functional data of amplitude and beat rate of the cardiomyocytes. Differentiation of these hiPSC lines into cardiomyocytes, followed by drug treatment, will allow the hiPSC-derived cardiomyocytes to act as *in vitro* cardiovascular safety models of genetic variability. This can help understanding of the impact of genetic variability and its role in drug-induced cardiotoxicity.

Keywords: hiPSCs, CRISPR/Cas9, RYR2, cardiotoxicity

Acknowledgements

I want to thank Linda Starnes at AstraZeneca for sharing your knowledge and expertise in the subject. You have been a great supervisor in teaching me laboratory methods as well as giving me invaluable feedback regarding the report. This thesis would not have been possible without your guidance.

I want to thank Amy Pointon and the In Vitro Cardiovascular Safety Group at AstraZeneca for giving me the opportunity to perform my thesis as part of the team and for giving me further insight into the area.

I want to thank AstraZeneca for sharing know-how and providing me with all the equipment needed to make this thesis possible and for a great work environment.

I want to thank GATC Biotech for performing Sanger sequencing of the DNA from all the cell lines achieved in this thesis and Cell Guidance Systems for performing karyotype analysis of cell lines investigated in this thesis.

I want to thank Julie Gold at the Department of Physics at Chalmers University of Technology for being the examiner of this thesis and for providing me with feedback and advice.

Finally, I want to thank my family and friends for all the support and motivation you have given me throughout the thesis.

Michelle Kha

Gothenburg, January 2019

Table of contents

List of abbreviations

ARVD	arrhythmogenic right ventricular dysplasia
BSA	bovine serum albumin
Cas9	clustered regularly interspaced palindromic repeat-associated protein 9
CPVT	catecholaminergic polymorphic ventricular tachycardia
CRISPR	clustered regularly interspaced short palindromic repeats
crRNAs	clustered regularly interspaced short palindromic repeats RNAs
cTnT	cardiac troponin T
dbSNP	Single Nucleotide Polymorphism database
DSB	double strand break
FACS	fluorescence-activated cell sorting
GFP	green fluorescent protein
gRNA	guideRNA
GSK3	glycogen synthase kinase 3
HDR	homology-directed repair
Het KO	heterozygous knock-out
hiPSC	human induced pluripotent stem cell
hiPSC-CMs	human induced pluripotent stem cell-derived cardiomyocytes
ICC	immunocytochemistry
iPSC	induced pluripotent stem cell
LTCC	L-type Ca^{2+} channel
NCBI	National Center of Biotechnology Information
NCX	Na^{+}/Ca^{2+} exchanger
NGS	Next Generation Sequencing
NHEJ	non-homologous end-joining
PAGE	polyacrylamide gel electrophoresis
PAM	protospacer adjacent motif
PBS	phosphate buffered saline
PLN	phospholamban
RYR2	ryanodine receptor 2
SDS-PAGE	sodium dodecyl sulfate-polyacrylamide gel electrophoresis
SEM	standard error of mean
SERCA2	sarcoplasmic reticulum Ca^{2+} ATPase 2
SNP	single nucleotide polymorphism
SR	sarcoplasmic reticulum
ssODN	single-stranded oligodeoxynucleotide
TALENs	transcription activator-like effector nucleases
TCF/LEF	T-cell factor/lymphoid enhancer-binding factor
tracrRNA	transactivating clustered regularly interspaced short palindromic repeats RNAs
TTCC	T-type Ca^{2+} channel
VGCC	voltage-gated calcium channel
WT	wild-type
ZFNs	zinc finger nucleases

1. Introduction

1.1. Background

Cardiotoxicity is the leading cause of drug attrition during clinical trials. About 45% of all drug failures during the past decades are due to cardiac adverse effects, including arrhythmia, stroke, heart failure, hypertension and hypotension [1,2]. Currently, preclinical trials are performed with *in vivo* studies of animal models or *in vitro* studies of human models based on healthy donor cells. Animal models can mimic human mechanisms to some extent, but they are not capable of providing a completely reliable result in humans. Therefore, animal testing is hard to justify from an ethical perspective. Human *in vitro* modeling needs to be improved by implementation of studies considering disease aspects. This is required for improved understanding of the translation of important safety liabilities from healthy to disease states [3]. Patient-centric *in vitro* cardiovascular models can be created by gene modification of human induced pluripotent stem cells (hiPSCs), to mimic natural mutations in the human population, followed by differentiation into cardiomyocytes [4]. The development of patient-centric models is central for understanding of patient-specific risks, which is key to providing safe and efficacious drugs.

1.2. Aim

The over-arching aim of this thesis is to establish patient-centric *in vitro* cardiovascular models of genetic variability within a key calcium handling gene, *RYR2*, and to establish what impact this has for testing of drugs and development of drug-induced cardiotoxicity. Since the thesis is divided into two parts, there are two sub aims. The aim of the first part of the thesis is the creation of an iPSC line with the heterozygous single nucleotide polymorphism (SNP) rs3766871 (G1886S) within the *RYR2* gene that has been associated with cardiac diseases [5,6]. The aim of the second part is to characterize and differentiate an existing heterozygous knock-out (Het KO) iPSC line into cardiomyocytes. This will create a cardiovascular model of reduced RYR2 expression and understanding of its impact on drug responses and development of cardiotoxicity. The knock-out within the *RYR2* gene is a way to mimic the partial reduction in RYR2 expression seen in aging and heart disease [7-11]. The work in this thesis is a step towards personalized medicine which will result in reduced animal testing as well as shortening of the timeline in drug discovery.

2. Theory

In this section, the theoretical background of cardiac muscle and its function will be outlined as well as the current knowledge of *RYR2* mutations and their associations to cardiac diseases. The differentiation of hiPSCs into cardiomyocytes will be presented and explained. Furthermore, descriptions of the methods used in the thesis will be given.

2.1. Cardiac muscle and contraction

Cardiac muscle is found in the walls of the heart. Blood is pumped throughout the whole body by the contractions of the cardiac muscle in the left ventricular wall of the heart. Cardiac muscle consists of cardiomyocytes surrounded by a loose connective tissue matrix, which is connected to the fibrous cardiac skeleton, and a high abundance of blood vessels. The cardiomyocytes are connected by intercalated discs composed of desmosomes and gap junctions. The desmosomes keep the cells connected during contraction, while the gap junctions allow ions to be transferred between the cells resulting in current transmission across the heart. This results in a synchronous contraction of the whole heart as a unit. The volume of a cardiomyocyte is mainly occupied by mitochondria and myofibrils composed of sarcomeres. The sarcomeres are in turn composed of myofilaments; thin actin filaments and thick myosin filaments [12]. The structure of cardiac muscle is illustrated in Figure 1.

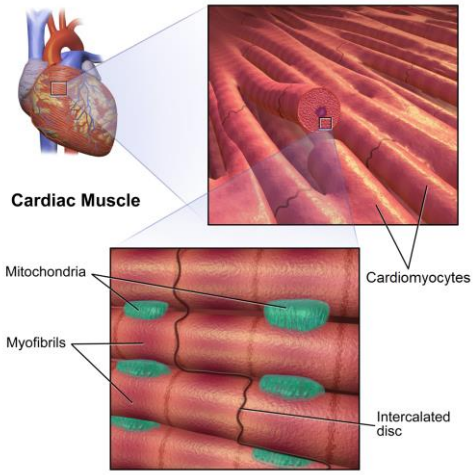

Figure 1. Structure and composition of cardiac muscle. Available from: https://upload.wikimedia.org/wikipedia/commons/7/73/Cardiac_Muscle.png.

Cardiomyocyte contraction is controlled by the transfer of Ca^{2+} in and out of the cell as well as between the sarcoplasmic reticulum (SR) and the cytosol. The Ca^{2+} channels that allow entry of Ca^{2+} into the cell, known as voltage-gated Ca^{2+} channels (VGCCs), can be divided into two different types, the L-type Ca^{2+} channels (LTCCs) and the T-type Ca^{2+} channels (TTCCs). The LTCCs are referred to as "L" due to their long-lasting inward current and slow decay, while the "T" in TTCCs refers to the transient inward current and rapid decay of the channels [13,14]. In response to the voltage change caused by Na^{+} influx from depolarization, Ca^{2+} ions get transferred into the cytosol through LTCCs [12]. These Ca^{2+} ions bind to and activate the ryanodine receptor 2 (RYR2) [13]. RYR2 is a large Ca^{2+} release channel found in the SR membrane which releases Ca^{2+} to the cytosol upon activation [3,13,15]. The following increase in cytosolic Ca^{2+} causes Ca^{2+} ions to bind to troponin which allows myosin to bind to actin. The binding causes the actin filament to move to the center of the sarcomere, resulting in muscle contraction. Muscle relaxation occurs by Ca^{2+} removal from the cytosol. The two main mechanisms for Ca^{2+} removal include the SR Ca^{2+} ATPase 2 (SERCA2), which transports Ca^{2+} from the cytosol to the SR, and the Na^{+}/Ca^{2+} exchanger (NCX), which pumps Ca^{2+} out of the cell [13]. The components involved in cardiac contraction are depicted in Figure 2.

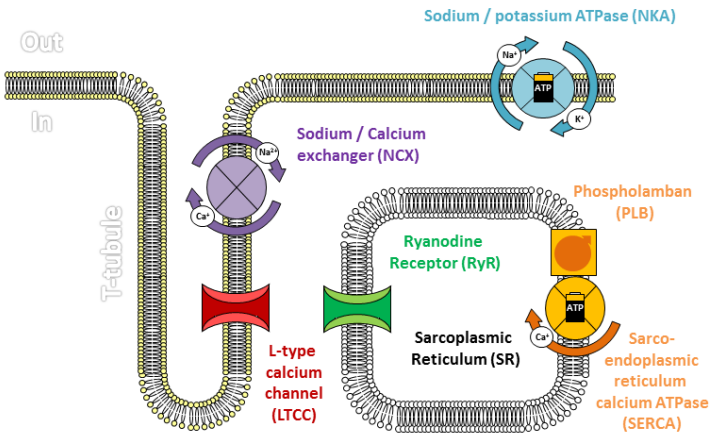

Figure 2. Components involved in cardiac contraction. Available from: https://upload.wikimedia.org/wikipedia/commons/1/10/Cardiac_calcium_cycling_and_excitation-contraction_coupling.png

2.2. RYR mutations

There are three different isoforms of RYR. RYR1 is mainly found in skeletal muscle, RYR2 in the heart and RYR3 in the brain. >300 *RYR* mutations are associated with diseases. Examples of cardiac diseases that are linked to *RYR2* mutations include catecholaminergic polymorphic ventricular tachycardia (CPVT) and arrhythmogenic right ventricular dysplasia (ARVD). CPVT gets triggered by emotional or physical stress while patients with ARVD have fibrofatty replacements in the right ventricular myocardium, both conditions resulting in arrhythmia [16]. In addition, there are mutations within the *RYR2* gene that are annotated benign according to the Single Nucleotide Polymorphism database (dbSNP) of the National Center of Biotechnology Information (NCBI), although associations with cardiac diseases have been found. Two of these mutations are the rs3766871 (G1886S) and rs41315858 (G1885E) variants. G1886S is the second most common heterozygous SNP within *RYR2*, followed by G1885E [17]. The two SNPs in combination have been associated with ARVD [5]. G1886S alone has been linked to ventricular arrhythmias and sudden cardiac death in chronic heart failure [6]. These findings have proposed an interest for the G1886S mutation, hereafter called SNP1, which one part of the thesis will focus on. There is a low likelihood of success in obtaining the SNP1 mutation, due to reasons that are further explained in the next section. Consequently, there is a second part of the thesis which will focus on a heterozygous knock-out mutation, since a partial reduction in RYR2 expression has been observed in aging and heart disease [7-10].

2.3. Differentiation of hiPSCs into cardiomyocytes

Human iPSCs are capable of differentiation into all somatic cells of a body. To direct the iPSCs towards a specific cell fate, the iPSCs need to be provided with developmental cues. One of the Wnt signaling pathways, namely the canonical Wnt pathway, has shown to be a key regulator of cardiogenesis and is consequently central for differentiation into cardiomyocytes. Wnt is promoted by inhibition of glycogen synthase kinase 3 (GSK3). This results in accumulation of β-catenin which activates gene transcription together with T-cell factor/lymphoid enhancer-binding factor (TCF/LEF). The canonical Wnt pathway is visualized in Figure 3.

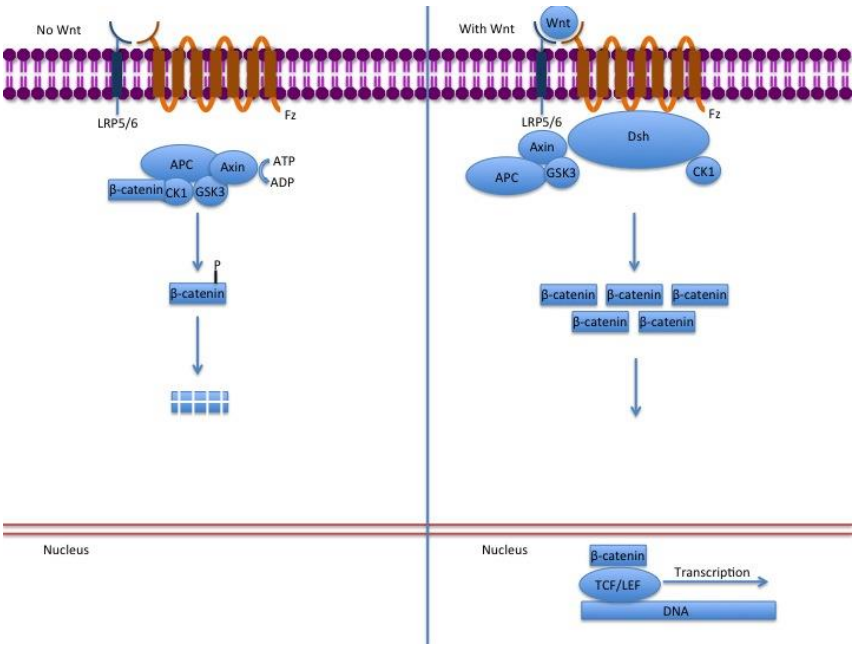

Figure 3. Canonical Wnt pathway. To the left, β-catenin is degraded by a destruction complex in the absence of Wnt. To the right, β-catenin accumulates in the presence of Wnt. Available from: https://upload.wikimedia.org/wikipedia/commons/6/6c/Canonical_Wnt_pathway.jpg

Differentiation of iPSCs into cardiomyocytes have been found to be directed by regulation of the canonical Wnt pathway. Addition of GSK3 inhibitor has shown to stimulate Wnt signaling and induce differentiation towards mesoderm cells. Subsequently, addition of the growth factor activin A causes knockdown of β-catenin expression which further promotes cardiogenesis. An essential last step to direct the differentiation towards cardiac progenitor cells is the addition of Wnt pathway inhibitor which blocks Wnt protein secretion and activity. The cells are cultured in RPMI/B27 medium during the whole differentiation process [18].

2.4. CRISPR/Cas9

Clustered regularly interspaced short palindromic repeats (CRISPR) systems are adaptive immune mechanisms found in bacteria and archaea. They are originally used for protection against foreign nucleic acids in the form of viruses and plasmids. The system works by incorporating sequences of the foreign DNA into the CRISPR repeat sequences which will subsequently be transcribed to CRISPR RNAs (crRNAs). Each crRNA consists of a part of a CRISPR repeat and a protospacer sequence, a sequence transcribed from the foreign DNA. The crRNA hybridizes with a non-coding transactivating crRNA (tracrRNA) and the protospacer region of the RNA hybrid directs the CRISPR associated protein 9 (Cas9) nuclease to cleave complementary DNA sequences if they are close to short sequences known as protospacer adjacent motifs (PAMs). PAM sequences are only found in the invading virus or plasmid which prevents self-targeting by the CRISPR system [19,20].

In the past decade, the type II CRISPR system from *Streptococcus pyogenes* has been adapted to be used for targeted genome editing [19]. Namely, CRISPR/Cas9 has shown to be a promising tool for single-base-pair gene editing in iPSCs, allowing creation of *in vitro* models of human diseases [21]. The two main components of the CRISPR/Cas9 system are Cas9 and guideRNA (gRNA), a fusion of a crRNA and a constant tracrRNA. The first 20 nucleotides of the gRNA correspond to the protospacer sequence of the crRNA and must lie immediately 5' of a PAM sequence in the form of NGG. This means that these 20 nucleotides can be altered to target any DNA sequence of the form N_{20}-NGG for cleavage by Cas9 since it will recognize the PAM sequence and consequently introduce a double-strand break (DSB) 3 bp upstream of the PAM [20,22]. DSBs are usually repaired via the non-homologous end-joining (NHEJ) pathway which results in non-specific insertions and deletions, so called "indels". This will generate gene knock-outs by introducing a shift in the reading frame of the gene. To generate a site-specific sequence change, homology-directed repair (HDR) is required. HDR within hiPSCs occurs in 1-10% of all editing events versus 90-99% for NHEJ. HDR can be achieved by introducing a single-stranded oligodeoxynucleotide (ssODN), containing the desired sequence change as well as homologous sequences to the targeted genomic region. Furthermore, NHEJ repair can be prevented by improvement of cell cycle manipulations, inhibition of NHEJ components, prevention of re-editing or specific design of repair templates. Prevention of re-editing can be obtained by introducing a silent mutation in the PAM site, preventing subsequent detection of the PAM site by Cas9 [22]. In addition, by introducing mixed repair templates, in the form of wild-type (WT) ssODNs, including only the silent mutation of the PAM site, and ssODNs including both the silent mutation of the PAM site as well as the desired site-specific sequence change, a heterozygous introduction of the sequence change can be obtained [21]. The whole process of cleavage and DNA repair by the CRISPR/Cas9 system is visualized in Figure 4.

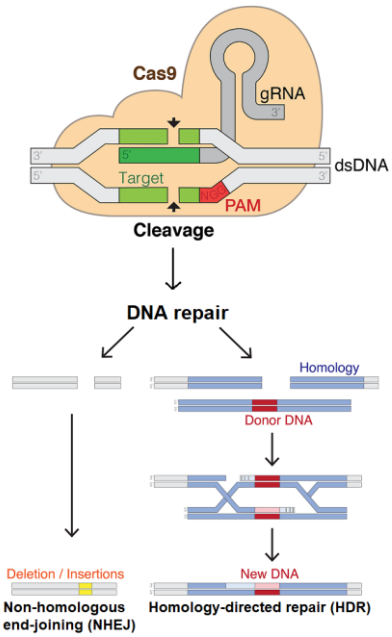

Figure 4. The process of CRISPR/Cas9 including cleavage and two types of DNA repair; non-homologous end-joining (NHEJ) and homology-directed repair (HDR). Available from: https://upload.wikimedia.org/wikipedia/commons/0/0c/DNA_Repair.png.

Apart from CRISPR/Cas9, there is a number of early gene editing methods. These include meganucleases, zinc finger nucleases (ZFNs) and transcription activator-like effector nucleases (TALENs). All four methods are based on customization of DSB-inducing nucleases for targeting of specific genomic sites. Meganucleases are engineered restriction enzymes with extended DNA recognition sequences. The DNA recognition and cleavage functions are intertwined in a single domain making it a challenge to modify the target DNA specificity of the nucleases. In contrast, ZFNs and TALENs are fusion proteins of an engineered DNA binding domain and a non-specific cleavage from the FokI restriction enzyme, thereby making it simpler to customize the DNA binding domain. However, ZFNs have a limited targeting capability, whereas the design and construction of TALENs have shown to be time-consuming and costly. Another challenge with TALENs is the delivery of the constructs, since the TALEN-coding sequences are large and highly repetitive. Due to the limitations of these early gene editing methods, the current research within gene editing is focusing on CRISPR/Cas9 [19,20,23].

2.5. Fluorescence-activated cell sorting

Fluorescence-activated cell sorting (FACS) is based on the technique of flow cytometry which involves optical analysis of biological particles or cells within a fluid stream passing through a light source, by measurement of the absorption and scatter of light [24]. In FACS, cells are fluorescently labeled either by transfection with expression constructs encoding fluorescent proteins, e.g. green fluorescent protein (GFP), or introduction of antibodies coupled to a fluorescent dye that bind specifically to the cells of interest [24,25]. This will allow labeled cells to be separated from unlabeled ones. The separation is obtained by introducing the cells into a fluid stream passing through a laser beam and measuring the fluorescence of the cells. A vibrating nozzle generates droplets of single cells or no cells which are given a positive or a negative charge depending on whether the cells are fluorescent. Droplets containing multiple cells are detected by increased light scatter and do not get charged. Subsequently, the droplets pass by an electric field which directs the droplets into different containers depending on their charge. The cell sorting occurs at a speed of several thousand cells per second [25].

2.6. Surveyor nuclease assay

Surveyor nuclease is an enzyme isolated from celery, also known as CEL I nuclease. It is used for mutation detection since it can detect and cut DNA at sites of base-substitution mismatches. To use the Surveyor nuclease for mutation detection, the target DNA needs to be amplified by PCR, followed by hybridization to form heteroduplexes. The Surveyor nuclease recognizes mutations and cleaves both strands of the heteroduplexes, resulting in cleavage products that can be analyzed using polyacrylamide gel electrophoresis (PAGE) where the cleavage products will be separated by size. The samples containing cleavage products indicates sequences with a mutation site. Consequently, the Surveyor nuclease assay provides a method for mutation screening without generation of unnecessary sequencing data [26]. Figure 5 depicts the process of the Surveyor nuclease assay.

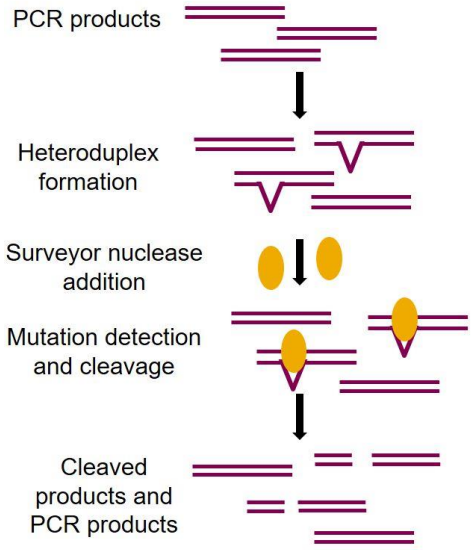

Figure 5. The process of the Surveyor nuclease assay for mutation detection.

2.7. Sanger sequencing

Sanger sequencing is one of the earliest methods for DNA sequencing. It is based on the DNA synthesis process and makes use of dideoxynucleotides which are chemically modified nucleotides. The DNA sequence of interest acts as a template for DNA synthesis of a new chain. Normal deoxynucleotides are mixed with a smaller amount of dideoxynucleotides which allows the dideoxynucleotides to be randomly incorporated into the new DNA chain. Once a dideoxynucleotide gets incorporated, the DNA synthesis process stops due to the lack of hydroxyl group at the 3' end. Four separate DNA synthesis reactions with dideoxynucleotides of each base occurs simultaneously using the same DNA sequence as a template. This will result in DNA chains of various lengths, differing by one base, which are complementary to the DNA template. The DNA chains are separated with electrophoresis with each lane representing each DNA synthesis reaction. Consequently, each lane will only contain DNA chains terminated with one specific base. The sequence can be determined by reading from the bottom of the gel, since the band with the shortest length will have migrated the furthest, and the base is determined by which lane the band is found [25,27].

2.8. Immunocytochemistry

Immunocytochemistry (ICC) is a method to examine proteins and molecules in cells using antibodies. The cells are prepared for ICC analysis by fixation to prevent degeneration. Fixation occurs by addition of chemicals with aldehyde groups that crosslink molecules

within the cell. To allow antibodies to bind to antigens within the cells, the cells are permeabilized by addition of detergents to open the membrane of the cell. Antibodies can bind non-specifically to charged groups on proteins or lipids and Fc receptors found on macrophages and other immune cells. Consequently, blocking agents for each of these non-specific binding sites need to be added. The most common blocking agent to prevent non-specific binding to charged groups is bovine serum albumin (BSA). The Fc receptors are blocked with IgG molecules which are usually obtained by addition of 10% normal serum from the same species of the secondary antibody [28]. After the addition of blocking agents, the primary antibody can be added, followed by addition of the secondary antibody. The primary antibody will bind to the molecule of interest, while the secondary antibody will bind to the primary antibody. The secondary antibody is coupled to a marker molecule which will allow detection of the target molecule. The choice of marker molecule will decide the method of detection, e.g. fluorescent dyes are analyzed by fluorescence microscopy and enzymes, that allow generation of a colored reaction product, are analyzed by conventional light microscopy or electron microscopy [25].

2.9. Western blotting

Western blotting is a procedure to detect specific proteins by exposure to an antibody labeled with a radioactive isotope, a detectable enzyme or a fluorescent dye. It is typically carried out after separation of the proteins by sodium dodecyl sulfate-polyacrylamide gel electrophoresis (SDS-PAGE). SDS-PAGE separates proteins by size by firstly exposing the proteins to the highly negative solution SDS, which binds to the hydrophobic regions of the protein, resulting in unfolded proteins. Secondly, the protein solution is run on a highly crosslinked polyacrylamide gel with an applied electric field causing the proteins to migrate at differing rates depending on the size of the protein. In Western blotting, the proteins in the gel from SDS-PAGE are transferred (or "blotted") onto a sheet of nitrocellulose paper or nylon membrane by placing the sheet over the gel and applying an electric field to it. Thereafter, the sheet can be exposed to a solution containing labeled antibodies for detection of the protein of interest [25].

3. Materials and methods

In this section, the materials and methods used to carry out the experiment for this thesis will be presented. First, the procedure to obtain the SNP1 line will be described including the process of validating the genotype. This will be followed by a description of characterization of the Het KO line prior to and after cardiomyocyte differentiation.

3.1. SNP1 line

The methods described in this section were carried out to obtain and validate hiPSC lines with the SNP1 mutation, including transfection, single cell sorting, cell expansion and culture as well as screening of the genotype of the cell lines. The process of the SNP1 line is illustrated in Figure 6.

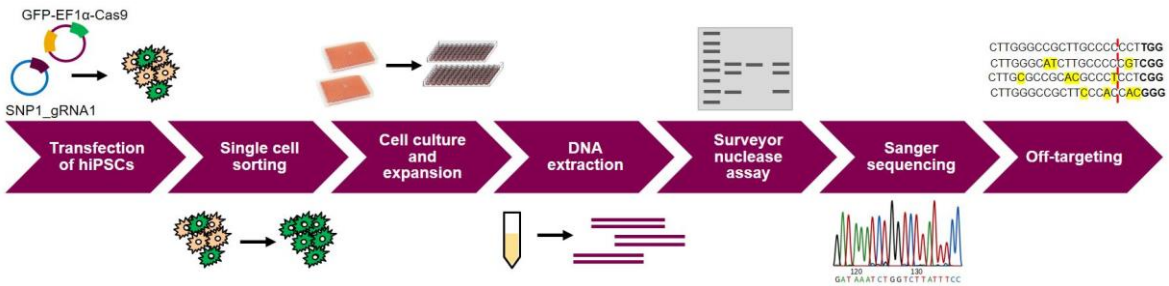

Figure 6. Flowchart of the process of the SNP1 line.

3.1.1. Reverse transfection of hiPSCs

Reverse transfection of an in-house hiPSC line, RIPS-1J, was performed using CRISPR/Cas9 to obtain the SNP1 mutation. To promote the HDR pathway and to obtain a heterozygous mutation, mixed repair templates were introduced in the form of WT and SNP1 ssODNs. To further promote the HDR pathway, a silent mutation of the PAM site was introduced in both the WT and SNP1 ssODNs. This should prevent re-editing by Cas9 after its first cleavage, since Cas9 will not be able to recognize the mutated PAM site to introduce an additional cleavage. The transfection was performed with concentrations of 20 and 40 nM ssODNs, according to previous transfections performed in-house on the RIPS-1J hiPSC line. The ssODNs, the GFP-EF1α-Cas9 plasmid, including Cas9 as well as GFP to enable sorting of the cells after transfection, and SNP1_gRNA1 in pMlu_U6rpsLBSD plasmid, including the gRNA with the SNP1 mutation, were introduced by liposome transfection. The sequences of the ssODNs and the SNP1_gRNA1 are presented in Appendix A.

RIPS-1J p9 hiPSCs were obtained from the Stem & Primary Cell Team at AstraZeneca and cultured in DEF-CS Basal Medium with supplements GF-1 (3 µL/mL) and GF-2 (1 µL/mL) (Takara). A 12 well plate was coated with DEF-CS COAT-1 (Takara), diluted 1:10 with phosphate buffered saline including calcium and magnesium (PBS +/+) (ThermoFisher), and incubated at room temperature for 30 min. Two transfection mixtures were made, one with 40 nM of ssODNs (Sigma-Aldrich) and one with 20 nM, both with a 1:1 ratio of WT and SNP1 ssODNs. The transfection mixtures were prepared by mixing 200 µL Opti-MEM (ThermoFisher), 500 ng GFP-EF1α-Cas9 plasmid, 500 ng SNP1_gRNA1 in pMlu_U6rpsLBSD plasmid and either 20 or 40 nM of ssODNs for each well. 1 µl PLUS reagent (ThermoFisher) for each well was added to the transfection mixtures and the mixtures were incubated for 5 min. At last, 2.5 µl Lipofectamine LTX (ThermoFisher) for each well was added to the transfection mixtures. The coating was aspirated from the wells and the transfection mixtures were added to four wells for each mixture. After 30 min, 250 000 RIPS-1J p11 iPSCs were plated in each well with 1 mL of DEF-CS Basal Medium with supplements GF-1 (3 µL/mL), GF-2 (1 µL/mL) and GF-3 (1 µL/mL) (Takara). The media was changed 24 h after transfection.

3.1.2. Single cell sorting

The cells were sorted 48 h after transfection. The sorting was based on the hypothesis that the fluorescent cells that expressed GFP, i.e. the cells that had picked up the GFP-EF1α-Cas9 plasmid, had undergone transfection and gene editing. The cells that were transfected with 20 nM ssODNs and 40 nM ssODNs, respectively, were sorted separately. The sorting included one well with a bulk sample for each condition, consisting of a mixed population of 150-300 transfected cells, while the rest of the cells were single cell sorted into one well each. The purpose of the bulk sample was to obtain a faster growth compared to the single cells and therefore the bulk sample could be analyzed earlier using the Surveyor nuclease assay to ensure that gene editing occurred in the GFP positive cells. In addition, the bulk sample could be expanded and re-sorted as single cells to obtain additional cell lines, if no cell lines with the desired mutation were obtained from the first sorting.

Two 384 well plates were coated with 25 µL DEF-CS COAT-1, diluted 1:10 with PBS +/+, for each well and incubated at 37 °C for 30 min. The coating was aspirated and 40 µL of DEF-CS Basal Medium with supplements GF-1, GF-2 and GF-3 + 10 µM ROCK Inhibitor (Y-27632) (Merck) was added to each well. The plates were incubated at 37°C for an additional 30 min. The cells were harvested from the 12 well plate by adding 400 µL of TrypLE Select (ThermoFisher) to each well and incubating for 5 min at 37°C. 600 µL of

DEF-CS Basal Medium with supplements GF-1, GF-2 and GF-3 was added to each well to quench the reaction. The cell suspensions were transferred into Falcon tubes and centrifuged at 150 g for 3 min. The pellets were resuspended in 300 µL DEF-CS Basal Medium with supplements GF-1, GF-2 and GF-3 and transferred into FACS tubes. The cells in the FACS tubes were single cell sorted into the two 384 well plates, one plate for cells transfected with 40 nM ssODN and the other for cells transfected with 20 nM ssODN, using the Sony SH800 cell sorter.

3.1.3. Cell expansion and culture

Six days after sorting, wells with developing colonies were marked and 40 µL of fresh media was added to each these wells. After nine days, the media was exchanged daily and the plates were continually scanned for clone outgrowth. The cells were cultured in DEF-CS Basal Medium with supplements GF-1 (3 µL/mL) and GF-2 (1 µL/mL). When the cells were confluent, they were expanded 2-3-fold, i.e. 1 well of a 384 well plate → 1 well of a 96 well plate → 1 well of a 48 well plate → 2 wells of a 24 well plate → 2-3 wells of a 12 well plate. When the 12 well plate stage was reached, 1-2 wells were frozen for potential future cell expansion and 1 well was frozen for DNA extraction.

The cells were prepared for expansion by changing media 2 h prior passaging. The media was aspirated from the well and the well was washed with phosphate buffered saline without calcium and magnesium (PBS -/-) (ThermoFisher). TrypLE Select was added to the well and the plate was incubated at 37℃ for 4 min. The cells were dissociated by pipetting up and down 10 times. The cell suspension was transferred to a larger plate that had been coated with DEF-CS COAT-1, diluted 1:10 with PBS +/+, and filled with DEF-CS Basal Medium with supplements GF-1, GF-2 and GF-3, ensuring a 1:10 dilution of TrypLE Select. The volume used for each reagent is presented in Appendix B.

When the lines had reached the 12 well plate stage and had become confluent, they were prepared for freezing by changing media 2 h ahead. The pre-feed media consisted of DEF-CS Basal Medium with supplements GF-1 (3 µL/mL) and GF-2 (1 µL/mL) + 10 µM ROCK Inhibitor (Y-27632). The media was aspirated and the wells were firstly washed with 2 mL PBS -/- and thereafter 200 µL TrypLE Select. 400 µL TrypLE Select was added to each well and the plate was incubated at 37℃ for 5 min. The cells were dissociated by pipetting up and down 10 times. 400 µL DEF-CS Basal Medium with supplements GF-1, GF-2 and GF-3 was added to each well to quench the reaction and the cell suspension was pipetted up and down an additional 10 times. The cell suspensions in the wells to be frozen for potential future expansion were transferred to a Falcon tube, while the cell suspension for DNA extraction was transferred to an Eppendorf tube. The Falcon tube was centrifuged at 200 g for 5 min and the Eppendorf tube was centrifuged at 2 500 rpm for 3.5 min. The supernatant in the Falcon tube was aspirated and the cell pellet was resuspended in 1 mL 10% DMSO (Sigma-Aldrich) and 90% FBS (ThermoFisher) + 10 µM ROCK Inhibitor (Y-27632). The cell suspension was transferred into a cryovial and preserved at -80℃. The supernatant in the Eppendorf tube was aspirated and the cell pellet was stored at -20℃.

3.1.4. DNA extraction

DNA was extracted for each cell line to enable screening of the DNA for the desired SNP1 mutation. Firstly, the DNA was analyzed using the Surveyor nuclease assay to detect any mutations in the sequence of interest. The cell lines that were determined positive from the Surveyor nuclease assay were thereafter prepared for Sanger sequencing.

DNA was extracted from the cell pellets using the Gentra Puregene Cell Kit (Qiagen). The cell pellets were defrosted in room temperature and the tubes were vortexed at maximum speed. 300 µL of Cell Lysis Solution was added to each tube and mixed by pipetting up and down. 1.5 µL of RNase A Solution was added to each tube and the tubes were inverted 25 times. The tubes were incubated at 37℃ for 5 min. The samples were cooled to room temperature by putting them on ice for 1 min. 100 µL of Protein Precipitation Solution was added to each tube and the tubes were vortexed at high speed for 20 s. The samples were put on ice for 5 min before centrifuging at 14000 rpm for 10 min. The supernatant was transferred to a clean Eppendorf tube and 300 µL isopropanol (Sigma-Aldrich) was added to the tubes containing the supernatants. The samples were mixed by inverting the tubes gently 50 times. The tubes were centrifuged at 14000 rpm for 10 min at 4℃. The supernatant was discarded and the tube was completely drained on absorbent paper. 300 µL 70% ethanol (CCS Healthcare) was added to the tubes and the tubes were centrifuged at 14000 rpm for 5 min. The supernatant was discarded and the DNA was airdried at 56℃ for a few minutes. 30 µL of PCR Grade Water (Sigma-Aldrich) was added to each tube and the samples were incubated at 56℃ for 45 min, shaking at 500 rpm. The samples were spun down quickly and cooled at 4℃ overnight and stored at -20℃ until further analysis.

3.1.5. Screening of SNP1 lines by Surveyor nuclease assay and Sanger sequencing

The cell lines were screened for mutations by performing the Surveyor nuclease assay. The DNA from each cell line was PCR amplified with primers targeting the sequence of interest, i.e. the location of the SNP1 mutation. The PCR products formed heteroduplexes which were screened by the Surveyor nuclease. The Surveyor nuclease introduced a cleavage at the site of mutation resulting in samples with cleaved fragments and PCR products. The samples were analyzed by separating the DNA fragments on a gel. From the gels, cell lines that showed cleaved fragments were determined positive and prepared for Sanger sequencing by PCR amplification and purification. Sanger sequencing was performed by GATC Biotech.

The DNA samples were defrosted and the DNA concentration was measured using NanoDrop (ThermoFisher). The samples were prepared for PCR amplification by adding 125 ng DNA, 0.5 µL of 10 µM SNP1 forward primer, 0.5 µL of 10 µM SNP1 reverse primer, 5 µL 2x Phusion Flash High-Fidelity PCR Master Mix and PCR Grade Water to a final volume of 10 µL in a PCR tube, for each sample. The sequences of the SNP1 forward and reverse primer are presented in Appendix A. The PCR program, shown in Table 2, was run on C1000 Touch Thermal Cycler (Bio-Rad) for DNA amplification.

Table 1. PCR program for DNA amplification.

	Temperature	**Time**
Initial denaturation	98℃	90 s
Amplification (33x)	98℃	5 s
	62℃	5 s
	72℃	5 s
Final extension	72℃	90 s
	12℃	Hold ∞

The PCR program for DNA amplification was followed by a PCR program for heteroduplex formation, presented in Table 3.

Table 2. PCR program for heteroduplex formation.

Temperature	Time	Temperature ramp
95°C	10 min	
95°C to 85°C		-2°C/s
85°C	1 min	
85°C to 75°C		-0.3°C/s
75°C	1 min	
75°C to 65°C		-0.3°C/s
65°C	1 min	
65°C to 55°C		-0.3°C/s
55°C	1 min	
55°C to 45°C		-0.3°C/s
45°C	1 min	
45°C to 35°C		-0.3°C/s
35°C	1 min	
35°C to 25°C		-0.3°C/s
25°C	1 min	
4°C	Hold ∞	

1 µL Surveyor Nuclease S and 1 µL Surveyor Enhancer S, from the Surveyor Mutation Detection Kit for Standard Gel Electrophoresis (Integrated DNA Technologies), was added to each sample. The samples were incubated at 42°C for 40 min. 3 µL Novex Hi-Density TBE Sample Buffer (5x) (ThermoFisher) was added to each sample. 4 µL of 1 Kb Plus DNA Ladder (ThermoFisher) and 10 µL of each sample were loaded on Novex 10% TBE Gel (ThermoFisher) on the XCell SureLock Mini-Cell Electrophoresis System (ThermoFisher) and run with Novex TBE Running Buffer (ThermoFisher) at 200 V for 40 min. The gels were stained with two drops of Ethidium Bromide solution 0.07% (PanReac AppliChem) in Milli-Q water for 5 min. The gels were imaged using Gel Doc XR+ Gel Documentation System (Bio-Rad).

The samples that showed cleaved DNA fragments were PCR amplified with the program described in Table 2, but with 200 ng DNA, 2.5 µL of 10 µM SNP1 forward primer, 2.5 µL of 10 µM SNP1 reverse primer, 25 µL 2x Phusion Flash High-Fidelity PCR Master Mix and PCR Grade Water to a final volume of 50 µL, for each sample. The PCR products were purified by following the instructions for the QIAquick PCR Purification Kit (Qiagen). The samples were eluted with 30 µL PCR Grade Water, warmed to 50°C. The purified DNA was sent to GATC Biotech who sequenced the samples using Sanger sequencing using the SNP1 forward and reverse primers.

3.1.6. Off-target analysis

Possible off-targets of the gRNA used for transfection with CRISPR/Cas9 were identified by the in-house CRISPR3 tool and the Sanger institute CRISPR finder. The top four regions targeted by the gRNA that contained coding or regulatory sequences identified by both the tools mentioned above where gRNA had full PAM site complementarily and/or fewer than five mismatches with the target were chosen for Sanger sequencing. The regions of interest are presented in Table 4.

Table 3. Regions identified as possible off-targets of the gRNA used in CRISPR/Cas9 transfection, including the gene each region is found within, the number of mismatches for each region as well as the role of the encoded protein.

Gene	Number of mismatches	Role of protein
CHRFAM7A	3	Subunit of ion channel
CHRNA7	3	Subunit of ion channel
PLEC	4	Involved in cytoskeleton formation
KBTBD6	4	Involved in immune system

The DNA from the line that had the potential SNP1 mutation was PCR amplified and sequenced by following the same procedure as for all the lines that were considered positive from the Surveyor nuclease assay and sent for Sanger sequencing. In this case, primers of the genes presented in Table 4 were used and the annealing temperature of the PCR program was set to 65°C. The sequences of the targets and the primers are presented in Appendix C. After PCR purification, the samples were sent to GATC Biotech for sequencing using the forward primer of each gene. The sequences were compared to database sequences using NCBI's Nucleotide BLAST. BLAST calculated the statistical significance of matches after comparing the similarity of the sequences. Consequently, it enabled detection of mutations in the analyzed sequences.

3.2. Het KO line

The Het KO line is a hiPSC line with a heterozygous KO within *RYR2* that has been obtained previously in the project that this thesis is part of, by transfection of the in-house RIPS-1J hiPSC line. The methods presented in this section were carried out for the Het KO line for validation of the genomic stability and pluripotency of the cells in their stem cell state, differentiation of hiPSCs into cardiomyocytes and characterization of the hiPSC-derived cardiomyocytes (hiPSC-CMs). All the procedures described in this section were performed simultaneously for a WT line, i.e. the RIPS-1J hiPSC line, for comparison. The process is presented in Figure 7.

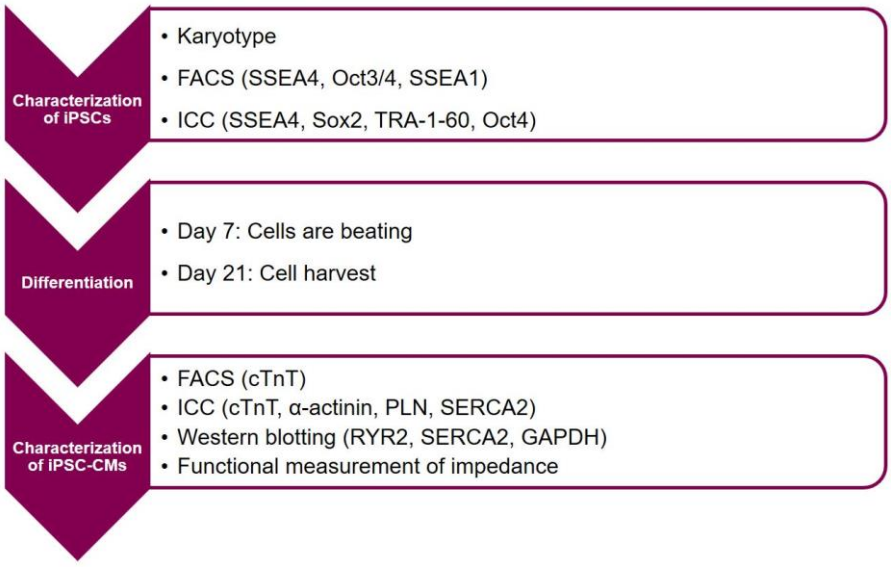

Figure 7. Flowchart of the process of the Het KO line.

3.2.1. iPS cell culture and passaging

The hiPSCs were cultured in DEF-CS Basal Medium with supplements GF-1 and GF-2 in a 6 well plate according to Takara DEF-CS Culture System instructions. The media was

changed daily and the cells were passaged every third day. For passaging, a 6 well plate was coated with DEF-CS COAT-1, diluted 1:20 with PBS -/-. The plate was incubated at 37℃ for 30 min or at room temperature for 30 min-3 h. The cells were firstly washed with 3 mL PBS -/- for each well and secondly 350 µL TrypLE Select. 700 µL TrypLE Select was added to each well and incubated at 37℃ for 5 min. The cells were dissociated by pipetting up and down 10 times. 700 µL DEF-CS Medium with supplements GF-1, GF-2 and GF-3 was added to each well and the cell suspension was pipetted up and down an additional 10 times. The cell suspension was added to a Falcon tube with 10 mL DEF-CS Medium with supplements GF-1, GF-2 and GF-3 and centrifuged at 200 g for 5 min. The supernatant was aspirated and the cell pellet was resuspended in 1 mL DEF-CS Medium with supplements GF-1, GF-2 and GF-3 before adding additional media to a total volume of 2 mL. The cell concentration was measured using Cedex HiRes Analyzer (Roche) and the cells were seeded at a density of 35 000-40 000 cells/cm^2 depending on their confluence when passaging.

3.2.2. Karyotype analysis of iPSCs

Karyotype analysis was performed to ensure the genomic stability of the hiPSC line. The cells were prepared for karyotype analysis by harvesting and fixing the cells during log phase, while the cells undergo cell division. The fixed cells were sent to Cell Guidance Systems who performed the karyotype analysis.

A T25 flask was coated with 2.5 mL BioLaminin 521 LN (BioLamina), diluted 1:10 with PBS +/+ to a concentration of 10 µg/mL and stored at 4℃ over the weekend. The flask was incubated at 37℃ for 1 h prior to seeding. The flask was washed with PBS -/- and 5 mL NutriStem hPSC XF Medium (Corning) was added to the flask. The cells were passaged as normal, but the cells were resuspended in 2 mL NutriStem hPSC XF Medium + 10 µM ROCK Inhibitor (Y-27632). The cell concentration was measured using Cedex HiRes Analyzer. 1 000 000 cells were seeded in the coated T25 flask. The media was changed daily.

After three days of culture, the media volume was adjusted to 6 mL. 65 µL of 10 µg/mL KaryoMAX Colcemid (ThermoFisher) was added to the flask and incubated at 37℃ for 1 h. 500 µL of FBS was added to a Falcon tube to act as a collecting tube for the cells. The media from the flask was transferred into the tube. 2.5 mL TrypLE Select was added to the flask. The flask was rocked gently for 10 s and the TrypLE Select was transferred to the collecting tube. An additional 2.5 mL TrypLE Select was added to the flask and incubated at 37℃ for 5 min. The cell suspension was pipetted up and down to produce a single cell suspension and thereafter transferred to the collecting tube. A final 1 mL TrypLE Select was added to the flask to wash off any residual cells and transferred to the collecting tube. The collecting tube was centrifuged at 900 rpm for 8 min. The supernatant was discarded and the cell pellet was dislodged by flicking the tube 20-30 times. 2 mL 0.075 M KCl (ThermoFisher) was added to the tube using a dropper while gently vortexing the tube. The total volume was adjusted to 4 mL with the same procedure. The tube was incubated at 37℃ for 25 min. 10 drops of 3:1 methanol (ThermoFisher)/acetic acid (Sigma-Aldrich) was added to the side of the tube using a dropper, letting the drops slide into the mixture slowly. The tube was inverted twice and incubated at room temperature for 10 min. The tube was centrifuged at 900 rpm for 8 min. The supernatant was discarded and the cell pellet was dislodged by flicking the tube 20-30 times. 2 mL of 3:1 methanol/acetic acid was added to the tube slowly while vortexing gently. The total volume was adjusted to 4 mL with the same procedure. The tube was inverted twice and incubated at room temperature for 30 min. The tube was centrifuged at 900 rpm for 8 min. The supernatant was discarded and the cell

pellet was dislodged by flicking the tube 20-30 times. 1.5 mL of 3:1 methanol/acetic acid was added to the tube and the tube was swirled to mix. The centrifugation and resuspension steps were repeated twice. The cell suspension was transferred to a 2 mL screw cap microcentrifuge tube. The tube was sealed with parafilm and stored in 4℃ before shipment to Cell Guidance Systems who proceeded with the remaining steps of karyotype analysis.

3.2.3. Pluripotency analysis of iPSCs by FACS

The pluripotency of the iPSCs was validated by analyzing the expression of pluripotency and differentiation markers, including cell surface proteins and intracellular transcription factors. The expression of the different markers was analyzed by addition of fluorochrome-conjugated antibodies which bound specifically to each of the markers. By performing FACS on the iPSCs, the fluorescence of each fluorochrome is measured and thereby pluripotent and differentiated cells can be distinguished based on their expression of each marker.

During regular cell passaging, 1 000 000 cells were added to a Falcon tube, with additional tubes for isotype control and unstained control. The tubes were centrifuged at 200 g for 5 min. The supernatant was aspirated and the cell pellets were resuspended in 200 µL 4% PFA (Sigma-Aldrich) in PBS -/-. The tubes were incubated at 4℃ for 30 min. 10 mL PBS -/- was added to each tube and the tubes was centrifuged at 500 g for 5 min. The supernatant was aspirated and the wash was repeated an additional two times. The cell pellets were resuspended in 5 mL PBS -/- and stored at 4℃ until FACS staining.

On the day of FACS analysis, cells were stained by following the instructions for the BD Stemflow Human and Mouse Pluripotent Stem Cell Analysis Kit (BD Biosciences). The cells and beads were resuspended in 300 µL of 2% FBS in PBS -/-, 2 mM EDTA and transferred to FACS tubes. The samples were placed on ice and run on the BD LSRFortessa (BD Biosciences) flow cytometer which separated the cells based on the measured fluorescence of each cell. The acquired data from FACS was analyzed in the flow cytometry data software FlowJo. The data was sorted based on the staining and gated to obtain graphical reports of the result.

3.2.4. Pluripotency analysis of iPSCs by ICC

The pluripotency of the iPSCs was further validated by ICC. The iPSCs were fixed to prevent degradation and permeabilized to allow analysis of intracellular pluripotency markers. A blocking agent was added to prevent non-specific binding of the antibodies, before the primary antibodies were added which bound to the pluripotency markers. This was followed by addition of secondary antibodies coupled to fluorescent dyes that bound to the primary antibodies. This allowed the pluripotency markers to be visualized by confocal microscopy.

A 96 well Greiner imaging plate was coated with 100 µL Geltrex (ThermoFisher), diluted 1:100 in DMEM (ThermoFisher), for each well. The plate was incubated in room temperature for 2 h. Cells were passaged as normal. 80 000 cells were taken from the cell suspension and diluted with mTeSR1 Basal Medium with supplement (STEMCELL Technologies) + 10 µM ROCK Inhibitor (Y-27632) to achieve a cell density of 50 cells/µL. 100 µL of the cell suspension was added in 10 wells, resulting in 5000 cells in each well. The media was changed daily.

After five days of culture, cells were fixed by adding 100 µL of 8% PFA in PBS -/- in each well, resulting in a final concentration of 4% PFA. The plate was incubated at room

temperature for 30 min. The wells were washed three times with 200 µL of PBS -/-. 200 µL PBS -/- was added to each well and the plate was stored at 4°C until staining.

The PBS -/- was aspirated and 100 µL 5% FBS and 0.1% Triton X-100 (Sigma-Aldrich) in PBS -/- was added to each well to permeabilize and block the cells. The plate was incubated at room temperature for 1 h. The wells were washed with 200 µL PBS -/- three times. The Embryonic Stem Cell Marker Panel (Abcam) was used as primary antibodies. The primary antibodies were combined as presented in Table 5 and diluted in blocking buffer consisting of 5% FBS in PBS -/-.

Table 4. Primary antibody combinations of pluripotency markers for ICC, including target protein, antibody host catalog number and dilution.

Combination	Antibody	Target protein	Antibody host	Catalog number	Dilution
1	SSEA4	Surface protein expressed in hPSCs	Mouse monoclonal	ab16287	1:100
	Sox2	Transcription factor expressed in hPSCs	Rabbit polyclonal	ab97959	1:1000
2	TRA-1-60	Surface protein expressed in hPSCs	Mouse monoclonal	ab16288	1:100
	Oct4	Transcription factor expressed in hPSCs	Rabbit monoclonal	ab19857	1:1000

80 µL of the two primary antibody combinations were added to each well. One well was left unstained to serve as negative control. The plate was incubated at 4°C overnight. The wells were washed with 200 µL PBS -/- three times before adding 100 µL of mixture containing secondary antibodies and Hoechst stain, diluted in blocking buffer, to each well including the negative control, see Table 6.

Table 5. Contents of mixture containing secondary antibodies and Hoechst stain for ICC, including dilution.

Stain	Dilution
Alexa Fluor 647, Goat anti-Mouse IgG (H+L), 2 mg/mL (ThermoFisher)	1:500
Alexa Fluor 568, Goat anti-Rabbit IgG (H+L), 2 mg/mL (ThermoFisher)	1:500
Hoechst 33342, Trihydrochloride, Trihydrate, 10 mg/mL (ThermoFisher)	1:5000

The plate was incubated in the dark at room temperature for 1 h. The wells were washed with 200 µL PBS -/- three times and filled with 200 µL PBS -/-. The plate was sealed with AbsorbMax film (Sigma-Aldrich) and imaged using the Cell Voyager 7000 (Yokogawa) microscope.

3.2.5. Differentiation of iPSCs into cardiomyocytes

The differentiation protocol of iPSCs into cardiomyocytes is based on the protocol of Lian et al. [18], involving regulation of Wnt signaling activity. The main steps include promotion of Wnt signaling to induce mesoderm development followed by inhibition of Wnt signaling to induce cardiac progenitor development. The protocol has been developed and optimized in-house by Linda Starnes and Caroline Hirst in the In Vitro Cardiovascular Safety Group at AstraZeneca.

Day 0
Each well of a 6 well plate was coated with 1.5 mL Geltrex, diluted 1:100 in DMEM. The plate was incubated at room temperature for 2 h. The Het KO iPSCs were cultured in a T75 flask in DEF-CS Basal Medium with supplements GF-1 and GF-2. The cells were firstly washed with 10 mL PBS -/- and secondly with 5 mL TrypLE Select. 5 mL TrypLE Select was added to the flask and the flask was incubated at 37°C for 5 min. The cell suspension was pipetted up and down 10 times and transferred into a Falcon tube with 30 mL DEF-CS Basal Medium with supplements GF-1, GF-2 and GF-3. The tube was centrifuged at 200 g for 5 min and resuspended in 1 mL DEF-CS Basal Medium with supplements GF-1, GF-2 and GF-3. An additional 2 mL of media was added to the tube. The cell concentration was measured using Cedex HiRes Analyzer. Additional media was added to the cell suspension to obtain a concentration of 700 000 cells/mL. 4 mL of the cell suspension was added to each well in the 6 well plate, resulting in 2 800 000 cells per well. After 2 h, the media was changed to 5 mL mesoderm induction media consisting of RPMI 1640 Medium GlutaMAX (ThermoFisher) with 100 µL B-27 Supplement (50X) minus vitamin A (ThermoFisher), 10 µM CHIR 99021 (Tocris), 50 µg/mL L-ascorbic acid (Sigma-Aldrich) and 8 ng/mL Activin A (Sigma-Aldrich) for each well.

Day 1
The media was changed to 5 mL cardiac mesoderm and progenitor induction media consisting of RPMI 1640 Medium GlutaMAX (ThermoFisher) with 100 µL B-27 Supplement (50X) minus vitamin A, 50 µg/mL L-ascorbic acid and 5 µM IWR-1 (Sigma-Aldrich) for each well.

Day 3
The media was changed to fresh cardiac mesoderm and progenitor induction media.

Day 5
The media was changed to 5 mL maintenance media consisting of RPMI 1640 Medium GlutaMAX (ThermoFisher) with 100 µL B-27 Supplement (50X) minus vitamin A and 50 µg/mL L-ascorbic acid for each well.

Day 7-20
The media was changed to fresh maintenance media every second day until harvest.

Day 21
The media was changed to fresh maintenance media + 10 µM ROCK Inhibitor (Y-27632) on the day of harvest. After 1 h, the wells were washed with 4 mL PBS -/- each. 800 µL of 0.25% Trypsin-EDTA, phenol red (ThermoFisher) was added in each well and the plate was incubated at 37°C for 4 min. The cells were dissociated by pipetting up and down 10 times and the plate was incubated for an additional 3 min. The reaction was quenched by transferring the cell suspension into a Falcon tube containing 20 mL EB20 medium consisting of KnockOut DMEM (ThermoFisher) with 20% FBS, 1 mM MEM Non-Essential Amino Acids Solution (ThermoFisher), 1 mM GlutaMAX Supplement (ThermoFisher) and 10 µM ROCK Inhibitor (Y-27632). The cell concentration was measured using Cedex HiRes Analyzer. The cells were aliquoted for different endpoints, as described in the following sections.

3.2.6. Characterization of iPSC-CMs by FACS

After differentiation, the iPSC-CMs were characterized by FACS by analyzing the expression of the cardiomyocyte marker cardiac troponin T (cTnT). The procedure was

similar to the procedure described for validation of pluripotency by FACS. However, only one fluorochrome-conjugated antibody bound to cTnT was added in this case. The fluorescence of the iPSC-CMs was measured to separate the cells based on cTnT expression.

500 000 cells were added to a Falcon tube, with additional tubes for isotype control and unstained control, and centrifuged at 200 g for 5 min. The supernatant was aspirated and the cell pellet was resuspended in 150 µL 4% PFA in PBS -/-. The tubes were incubated at 4°C for 30 min. The cells were washed with 5 mL PBS -/- twice. The cells were resuspended in 5 mL PBS -/- and stored at 4°C overnight. The following day the tubes were centrifuged at 500 g for 5 min. The supernatant was decanted and 1 mL Perm/Wash Buffer (BD Biosciences), diluted 1:10 in PBS -/-, was added in each tube. The tubes were centrifuged at 500 g for 5 min and the wash was repeated. The cells were resuspended in 1 mL Perm/Wash Buffer and the cell suspension was transferred to polystyrene tubes. The tubes were incubated in room temperature in the dark for 15 min. The tubes were centrifuged at 500 g for 5 min and the supernatant was decanted. 100 µL Anti-Cardiac Troponin T-APC (Miltenyi Biotec), diluted 1:100 in Perm/Wash Buffer, was added to the sample. 100 µL REA Control (I)-APC, diluted 1:100 in Perm/Wash Buffer, was added to the isotype control and the unstained control was left unstained. The tubes were incubated at room temperature in the dark for 45 min. 1 mL Perm/Wash Buffer was added to the tubes and the tubes were centrifuged at 500 g for 5 min. The wash was repeated twice. The supernatant was decanted and the cell pellets were resuspended in 300 µL of 2% FBS in PBS -/- + 2 mM EDTA and transferred to FACS tubes. The samples were placed on ice and run on the BD LSRFortessa flow cytometer which separated the cells based on the measured fluorescence of each cell. The acquired data from FACS was analyzed in the flow cytometry data software FlowJo. The data was sorted based on the staining and gated to obtain graphical reports of the result.

3.2.7. Characterization of iPSC-CMs by ICC

The iPSC-CMs were further characterized by ICC. The same procedure as for validation of pluripotency of the iPSCs was followed, but in this case, primary antibodies for cardiomyocyte markers were added instead. Apart from cTnT, the expression of three other cardiomyocyte markers were analyzed, including α-actinin, phospholamban (PLN) and SERCA2.

5 wells in a 384 well Greiner imaging plate were coated with 30 µL Geltrex, diluted 1:100 in DMEM, for each well. 20 000 cells were seeded in 50 µL of media for each well. After 24 h, cells were fixed by adding 50 µL 8% PFA in PBS -/- in each well, resulting in a final concentration of 4% PFA. The plate was incubated at room temperature for 20 min. The wells were washed three times with 100 µL of PBS -/-. 100 µL PBS -/- was added to each well and the plate was stored at 4°C until staining.

The PBS -/- was aspirated and 50 µL 5% FBS and 0.1% Triton X-100 in PBS -/- was added to each well to permeabilize and block the cells. The plate was incubated at room temperature for 1 h. The wells were washed with 50 µL PBS -/- three times. The primary antibodies were combined as presented in Table 7 and diluted in blocking buffer consisting of 5% FBS in PBS -/-.

Table 6. Primary antibody combinations of cardiomyocyte markers for ICC, including target protein, antibody host, catalog number and dilution.

Combination	Antibody	Target protein	Antibody host	Catalog number	Dilution
1	Anti-α-Actinin Antibody (Sigma-Aldrich)	Actin-binding protein	Mouse monoclonal	A7732	1:100
	Anti-Cardiac Troponin T Antibody (Abcam)	Tropomyosin-bound protein involved in regulation of contraction	Rabbit polyclonal	ab45932	1:500
2	Phospholamban Antibody (ThermoFisher)	Regulator of SERCA2	Mouse monoclonal	MA3-922	1:100
	Anti-SERCA2 ATPase Antibody (Abcam)	Enzyme involved in Ca^{2+} transport between cytosol and SR	Rabbit monoclonal	ab150435	1:300

40 µL of the two primary antibody combinations were added to each well. One well was left unstained to serve as negative control. The plate was incubated at 4℃ overnight. The wells were washed with 50 µL PBS -/- three times before adding 30 µL of mixture containing secondary antibodies and Hoechst stain, diluted in blocking buffer, to each well including the negative control, see Table 6. The plate was incubated in the dark at room temperature for 1 h. The wells were washed with 50 µL PBS -/- three times and filled with 50 µL PBS -/-. The plate was sealed with AbsorbMax film and imaged using the Cell Voyager 7000 microscope.

3.2.8. Characterization of iPSC-CMs by Western blotting

The Het KO line had a heterozygous KO in *RYR2* to mimic the partial reduction of RYR2 expression seen in aging and heart disease. Western blotting was performed to validate the knockdown of RYR2 to ensure its suitability as a model for reduced RYR2 expression. Western blotting was performed by lysing the iPSC-CMs to obtain the proteins of the cells. The protein was quantified by the Bradford assay to allow loading of the same amount of protein for all the analyzed samples in Western blotting. The proteins were separated by size by performing SDS-PAGE. Subsequently, the proteins were transferred onto a PVDF membrane. A blocking agent was added to the PVDF membrane before addition of the primary antibodies, which targeted the proteins of interest. Fluorescently labeled secondary antibodies were added which bound to the primary antibodies and allowed visualization of the proteins of interest.

1 000 000 cells were added to an Eppendorf tube and centrifuged at 2000 rpm for 3.5 min. The supernatant was aspirated and the cell pellet was resuspended in 100 µL RIPA Lysis and Extraction Buffer (ThermoFisher) with PhosSTOP (1 tablet/10 mL) (Roche) and cOmplete EDTA-free (1 tablet/10 mL) (Roche). The tube was put on ice for 30 min and inverted every 10 min before storing at -80℃.

The sample was defrosted and a Bradford assay was set up for protein quantification. Pierce Bovine Serum Albumin (ThermoFisher) standards were made by serially diluting the 2 mg/mL stock solution to obtain concentrations of 2, 1, 0.5, 0.25, 0.125, 0.063, 0.032 and 0 mg/mL. 5 µL of standards and samples that were diluted 1:4 with Milli-Q water, were added in duplicates to a 96 well plate. 300 µL of Pierce Coomassie (Bradford) Protein Assay Kit Solution (ThermoFisher) was added to each well. The plate was read on SpectraMax i3 Multi-Mode Microplate Detection Platform (Molecular Devices) at an absorbance of 595 nm.

20 µg of protein was added to an Eppendorf tube with NuPAGE LDS Sample Buffer (ThermoFisher), NuPAGE Sample Reducing Agent (ThermoFisher) and PCR Grade Water to a volume of 30 µL. The sample was boiled at 70°C for 10 min. 15 µL of HiMark Pre-Stained Protein Standard (ThermoFisher) and 30 µL of sample were loaded on NuPAGE 3-8% Tris-Acetate Protein Gel, 1.5 mm (ThermoFisher) on the XCell SureLock Mini-Cell Electrophoresis System and run with NuPAGE Tris-Acetate SDS Running Buffer (ThermoFisher) with 500 µL NuPAGE Antioxidant (ThermoFisher) at 120 V, 500 mA and 50 W for 1.5 h.

The PVDF membrane (ThermoFisher) was wetted in methanol and incubated in transfer buffer, consisting of 6.06 g Trizma base (Sigma-Aldrich), 28.8 g glycine (Bio-Rad), 400 mL methanol (Merck) in Milli-Q water of a total volume of 2 L, for 5 min while rocking. The Whatman papers and sponges were wetted in transfer buffer. The Western blot stack was set up and run in the Mini Trans-Blot Cell (Bio-Rad) with transfer buffer at 80 V for 85 min. The PVDF membrane was washed with TBS-T buffer (Tris buffered saline with Tween 20 tablet (Sigma-Aldrich) in 500 mL Milli-Q water). The membrane was cut into three different blots and blocked with 5% Skim Milk Powder (Sigma-Aldrich) in TBS-T buffer at room temperature for 1 h. Three primary antibody solutions were prepared in 5 mL of 5% Skim Milk Powder in TBS-T buffer each, as described in Table 8.

Table 7. Primary antibodies of cardiomyocyte markers for Western blotting, including target protein, antibody host, catalog number and dilution.

Antibody	Target protein	Antibody host	Catalog number	Dilution
Ryanodine Receptor Antibody (ThermoFisher)	Calcium channel	Mouse monoclonal	MA3-916	1:250
Anti-SERCA2 ATPase Antibody (Abcam)	Enzyme involved in Ca^{2+} transport between cytosol and SR	Rabbit monoclonal	ab150435	1:20 000
GAPDH Antibody (Cell Signaling Technology)	Actin-binding protein	Rabbit monoclonal	D16H11	1:5000

The blots were incubated in their designated primary antibody solution at 4°C overnight.

The blots were washed with TBS-T buffer for 5 min twice and for 10 min twice. Two secondary antibody solutions were prepared consisting of IRDye 800CW Goat anti-Mouse IgG (H+L) antibody (LI-COR) and IRDye 800CW Goat anti-Rabbit IgG (H+L) antibody (LI-COR), respectively, both diluted 1:15 000 in 20 mL of 10% Skim Milk Powder in TBS-T buffer each. The blots were incubated in their designated secondary antibody in dark at

room temperature for 1 h. The blots were washed with TBS-T buffer in dark for 10 min three times. The blots were imaged on the Odyssey CLx Imaging System (LI-COR).

3.2.9. Functional measurement of impedance of iPSC-CMs by CardioExcyte 96

The impedance of the iPSC-CMs was measured using the CardioExcyte 96 (Nanion Technologies. The system included a 96 well plate with embedded electrodes in the bottom which the iPSC-CMs were seeded in. The 96 well plate was placed in the incubation system, which enabled control of temperature, gas and humidity. The CardioExcyte 96 recorded the impedance and action potential of the iPSC-CMs. The recorded impedance acted as a surrogate measure of contractility, providing functional data of beat rate and amplitude of the iPSC-CMs.

A CardioExcyte 96 well plate (Nanion Technologies) was coated with 100 µL Geltrex, diluted 1:100 in DMEM, in each well. The cells were centrifuged at 200 g for 5 min. The media was aspirated and the cells were resuspended in maintenance media. 100 000 cells were seeded in 150 µL of media for each well. The media was changed every second day. On day 8, the impedance of the cells was measured using the CardioExcyte 96 while the cells were paced at 1 Hz. The impedance measurements provided data of beat rate and amplitude for each well. The data from eight wells for each cell line was analyzed in GraphPad Prism 7 and presented as mean ± standard error of mean (SEM).

4. Results

4.1. SNP1 line

A total of 43 lines from both conditions of 20 nM and 40 nM ssODNs, with a potential SNP1 mutation, were obtained from transfection and single cell sorting. The 43 lines correspond to survival of approximately 10% from the total number of single cells obtained after sorting. 39 of the lines showed cleaved DNA fragments in the result from the Surveyor nuclease assay. Figure 8 shows the result for lines 1-5 of the 40 nM lines, including a positive and a negative control. Figure 9 shows the result for lines 6-15 of the 40 nM lines, including lines that did not show any indications of mutation.

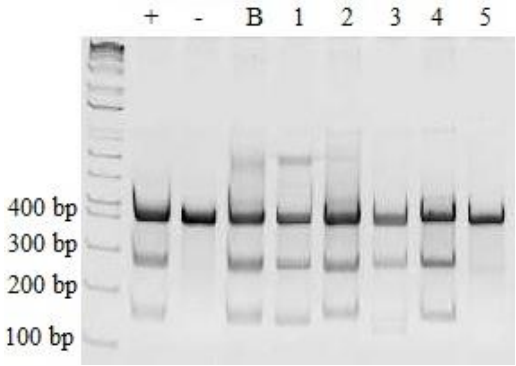

Figure 8. Gel from Surveyor nuclease assay including positive control (+), negative control (-), bulk sample (B) and lines 1-5 of the 40 nM lines. Lines 1-4 as well as the bulk sample are positive, whereas line 5 is negative.

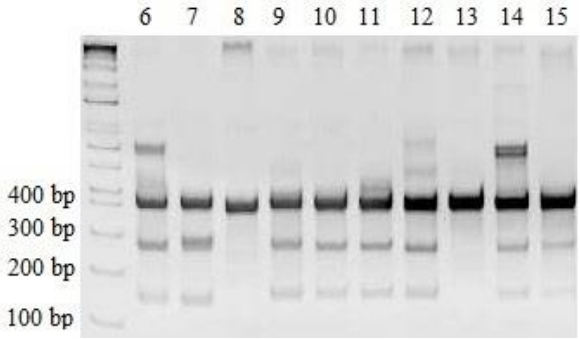

Figure 9. Gel from Surveyor nuclease assay including line 6-15 of the 40 nM lines. Lines 6-7, 9-12 and 14-15 are positive, whereas line 8 and 13 are negative.

As seen in Figure 8, the positive control (+) showed a dark band at 420 bp, with two smaller and lighter bands at 270 bp and 150 bp corresponding to the cleaved fragments of the sequence. The band of 420 bp corresponds to the sequence from forward to reverse primer, while the shorter bands correspond to the length from forward primer to the cleavage site as well as from the cleavage site to the reverse primer, see Appendix A. The negative control (-) only showed the dark band at 420 bp, indicating that no cleavage occurred. The lines that showed a band at 420 bp as well as bands around 290 bp and 270 bp, respectively, were considered positive, whereas lines that only showed a single band at around 420 bp were considered negative. The rest of the 40 nM lines as well as the 20 nM lines were determined accordingly. From Figure 8 and 9, cell lines 1-4, 6-7, 9-12 and 14-15 were determined positive. Cell line 5, 8 and 13 were determined negative. A summary of the results is listed in Table 9 and 10, with lines from transfection with 20 nM ssODNs and 40 nM ssODNs, respectively.

Table 8. Lines obtained from transfection with 20 nM ssODNs, including line name, passage number and date of freezing. The lines marked in red were determined negative based on the Surveyor nuclease assay.

Number	Line name	Passage number	Date of freezing
1	20-10	16	14/09/2018
2	20-5	16	15/09/2018
3	20-12	16	15/09/2018
4	20-3	16	16/09/2018
5	20-4	16	16/09/2018
6	20-6	16	16/09/2018
7	20-8	16	16/09/2018
8	20-11	16	16/09/2018
9	20-2	16	16/09/2018
10	20-13	16	16/09/2018
11	20-14	16	16/09/2018
12	20-7	16	18/09/2018
13	20-15	16	18/09/2018
14	20-16	17	20/09/2018
15	20-17	16	20/09/2018
16	20-18	16	20/09/2018
17	20-22	17	21/09/2018
18	20-21	17	21/09/2018
19	20-19	17	21/09/2018
20	20-23	17	21/09/2018
21	20-20	17	21/09/2018

Table 9. Lines obtained from transfection with 40 nM ssODNs, including line name, passage number and date of freezing. The lines marked in red were determined negative based on the Surveyor nuclease assay.

Number	Line name	Passage number	Date of freezing
1	40-1	16	14/09/2018
2	40-2	16	16/09/2018
3	40-3	16	16/09/2018
4	40-4	16	18/09/2018
5	40-5	16	18/09/2018
6	40-7	16	18/09/2018
7	40-6	16	18/09/2018
8	40-8	16	18/09/2018
9	40-11	16	18/09/2018
10	40-10	16	19/09/2018
11	40-12	16	19/09/2018
12	40-14	16	19/09/2018
13	40-19	16	20/09/2018
14	40-9	17	20/09/2018
15	40-13	17	20/09/2018
16	40-18	16	21/09/2018
17	40-8	16	21/09/2018
18	40-21	17	21/09/2018
19	40-10	17	21/09/2018
20	40-17	17	21/09/2018
21	40-15	17	23/09/2018
22	40-22	17	24/09/2018

From the 39 lines that were sent for sequencing, line 40-11 was the only line that appeared to have the desired mutation. The chromatograms from the sequence of interest from sequencing using the SNP1 forward and reverse primer are depicted in Figure 10 and 11, respectively. The full sequences are presented in Appendix D.

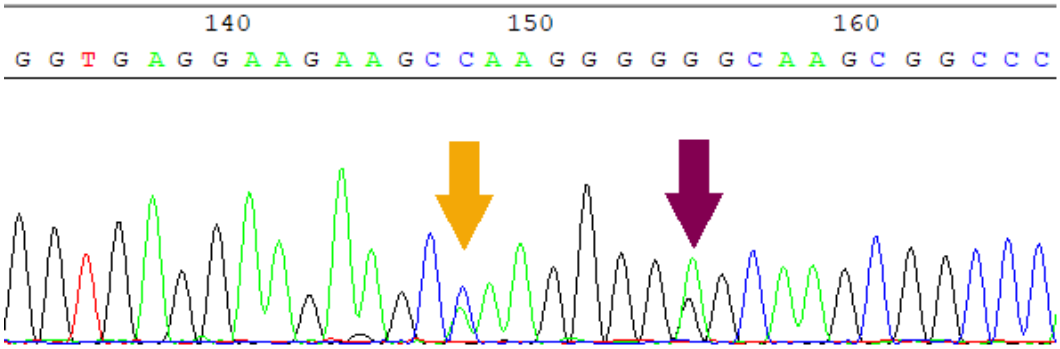

Figure 10. Part of chromatogram from sequencing of line 40-11 using the SNP1 forward primer. The orange arrow shows the silent mutation of the PAM site and the purple arrow shows the desired SNP1 mutation. G is visualized in black, A in green, T in red and C in blue.

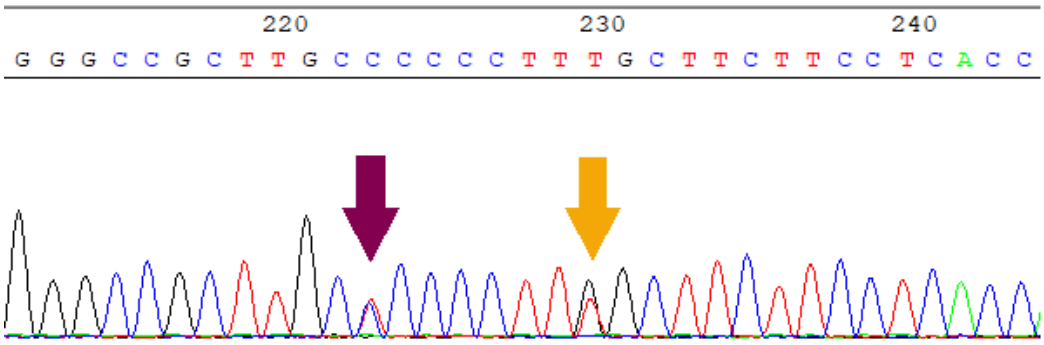

Figure 11. Part of chromatogram from sequencing of line 40-11 using the SNP1 reverse primer. The orange arrow shows the silent mutation of the PAM site and the purple arrow shows the desired SNP1 mutation. G is visualized in black, A in green, T in red and C in blue.

In Figure 10 and 11, the orange arrow shows the silent C>A mutation of the PAM site, which was incorporated to prevent re-editing by Cas9, while the purple arrow shows the desired G>A mutation to obtain the SNP1 mutation. As seen in Figure 10, there are peaks for both C and A at the site of the silent mutation as well as both G and A at the site of the SNP1 mutation. Correspondingly for the reverse strand seen in Figure 11, there are peaks for both G and T at the site of the silent mutation as well as C and T at the site of the SNP1 mutation. The presence of both WT and SNP1 peaks suggests a heterozygous SNP1 mutation with one allele conserving the WT sequence, whereas the other allele carries both the SNP1 mutation and the silent mutation of the PAM site.

Furthermore, line 40-11 was screened for off-target events. The sequencing result is presented in Figure 12.

Figure 12. Potential off-targets of line 40-11 that are complimentary with the gRNA with up to four mismatches. Regions located on the positive strand are presented to the left and the region located on the negative strand is presented to the right. The PAM sites are marked in bold and the dashed line indicates the potential Cas9 cleavage site. The only mismatch found is marked in red, but the mismatch was confirmed to be present in the WT line as well, as indicated in the figure.

As seen in Figure 12, no evidence for off-target events was detected in the top four coding regions that are complimentary to the gRNA with up to four mismatches. The only mismatch found was a SNP in the *KBTBD6* gene. However, the same SNP was present in the WT line suggesting that the SNP was present before transfection.

4.2. Het KO line

The results for the Het KO line are presented in two sections. The results from characterization of the iPSCs before differentiation, including karyotyping as well as validation of pluripotency by FACS and ICC, will be presented in one section. This will be followed by results from characterization of the iPSC-CMs after differentiation, including staining of cardiomyocyte markers and subsequent analysis by FACS and ICC as well as validation of RYR2 knockdown by Western blotting and functional measurement of impedance.

4.2.1. Characterization of iPSCs

The karyogram from the karyotype analysis of the WT and Het KO line is visualized in Figure 13 and 14, respectively.

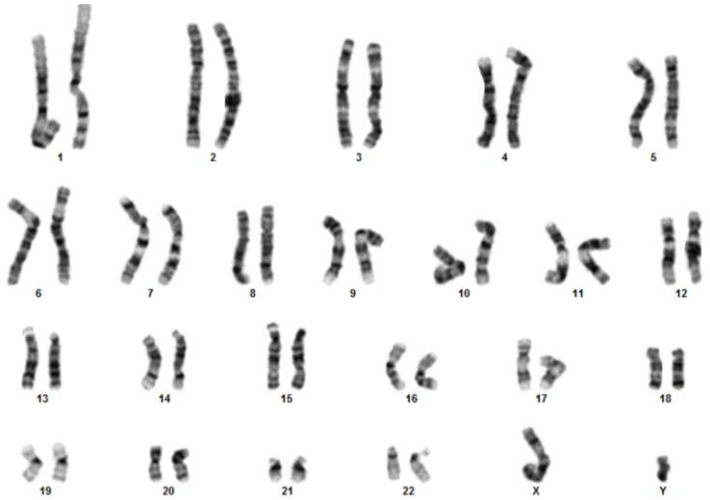

Figure 13. Karyogram of the WT line showing a normal male karyotype of 23 chromosome pairs.

Figure 14. Karyogram of the Het KO line showing a normal male karyotype of 23 chromosome pairs.

As seen in Figure 13 and 14, there are 22 pairs of autosomal chromosomes and one X chromosome and one Y chromosome, respectively, for both WT and the Het KO line. This indicates a normal male karyotype of 23 chromosome pairs of both cell lines.

The pluripotency of the iPSCs was validated by FACS by staining for the differentiation and pluripotency markers summarized in Table 11.

Table 10. Stains used for FACS analysis of iPSCs, listed with corresponding markers and target protein.

Stain	**Marker**	**Origin of protein**
PerCP-Cy5.5	Oct3/4	Transcription factor expressed in human pluripotent stem cells
PE	SSEA-1	Surface protein expressed in human differentiated cells
Alexa Fluor 647	SSEA-4	Surface protein expressed in human pluripotent stem cells

From Table 11, it can be concluded that the iPSCs should stain positive for Oct3/4 and SSEA-4, but stain negative for SSEA-1.

The results for WT and the Het KO line are presented in Figure 15 and 16, respectively.

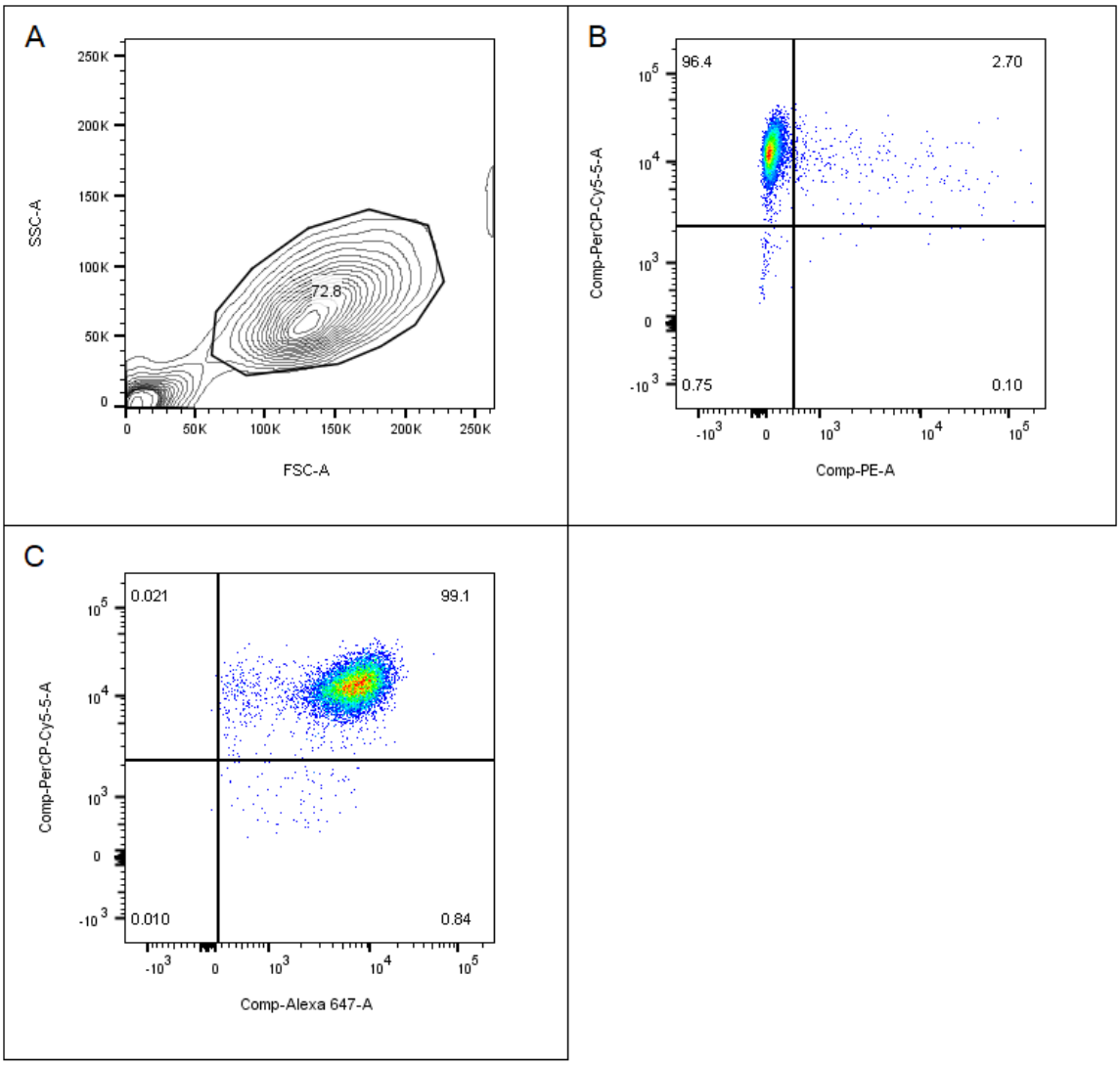

Figure 15. Validation of pluripotency for WT through FACS. Panel A shows an initial gating of live cells from the total population. In panel B and C, the gated cells are visualized in terms of SSEA-1 and Oct3/4 expression, and SSEA-4 and Oct3/4 expression, respectively.

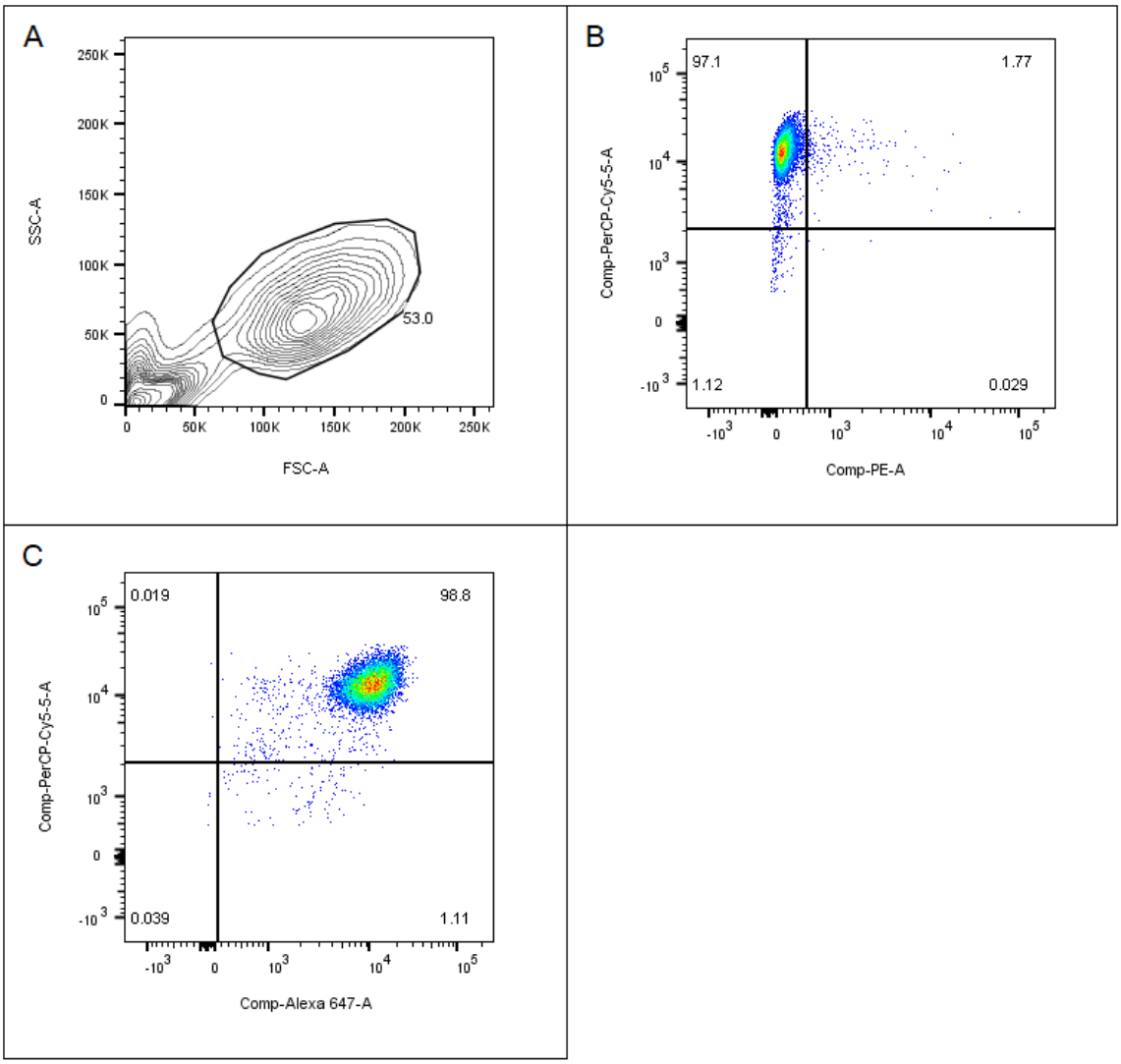

Figure 16. Validation of pluripotency for the Het KO line through FACS. Panel A shows an initial gating of live cells from the total population. In panel B and C, the gated cells are visualized in terms of SSEA-1 and Oct3/4 expression, and SSEA-4 and Oct3/4 expression, respectively.

As seen in Figure 15 and 16, approximately 97% of the population stained positive for Oct3/4 and negative for SSEA-1 for both WT and the Het KO line. In addition, 99% of both populations stained positive for both Oct3/4 and SSEA-4. The gates in panel B and C in Figure 15 and 16 were set based on the isotype control and validated with the unstained control to neglect any non-specific background staining or autofluorescence of the iPSCs, see Appendix E.

The pluripotency of the iPSCs was further confirmed through ICC. The results for WT and the Het KO line are presented in Figure 17 and 18 for SSEA4 and Sox2 as well as TRA-1-60 and Oct4, respectively.

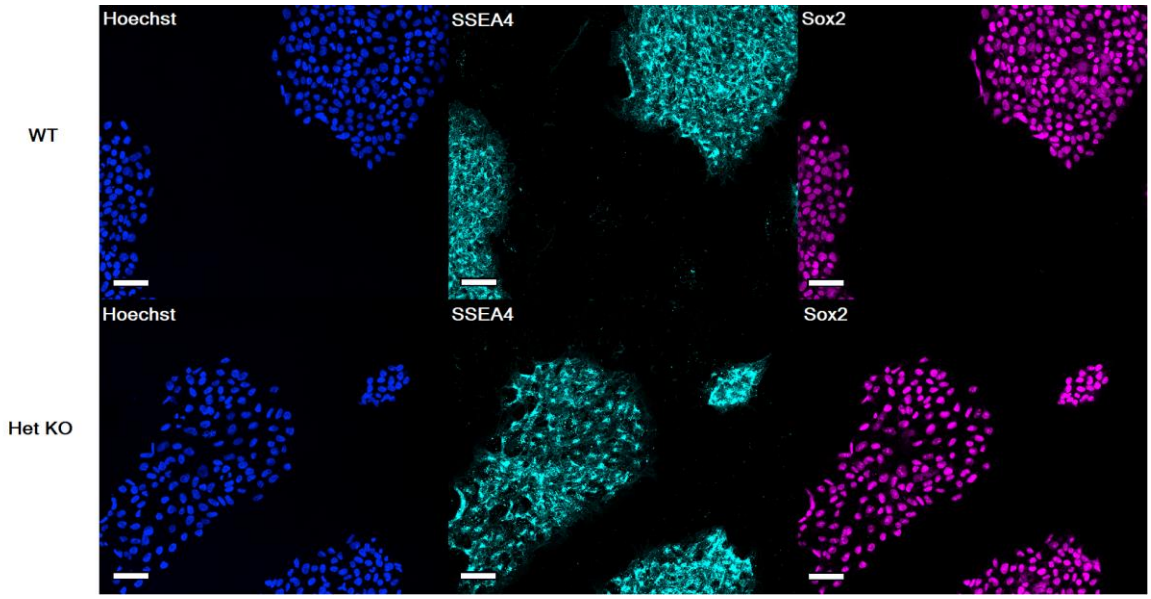

Figure 17. Validation of pluripotency for WT (upper row) and the Het KO (lower row) iPSCs through ICC. From left to right, DNA, i.e. cell nuclei, is visualized in blue, SSEA4 in cyan and Sox2 in magenta. The scalebar measures 100 µm.

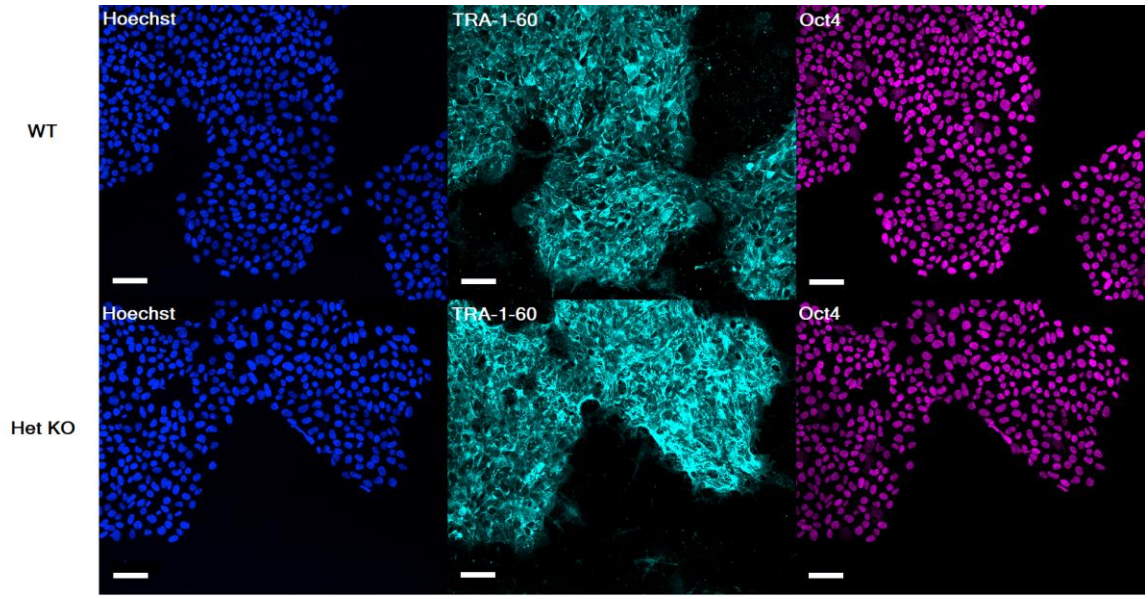

Figure 18. Validation of pluripotency for WT (upper row) and the Het KO (lower row) iPSCs through ICC. From left to right, DNA, i.e. cell nuclei, is visualized in blue, TRA-1-60 in cyan and Oct4 in magenta. The scalebar measures 100 µm.

As seen in Figure 17 and 18, both WT and the Het KO iPSCs stained positive for the pluripotency markers SSEA4, Sox2, TRA-1-60 and Oct4. Furthermore, the pluripotency markers were found where cell colonies were located, as indicated by the Hoechst stain in blue. The specificity of the stains was further validated by a negative control, see Appendix F.

4.2.2. Characterization of iPSC-CMs

The iPSC-CMs were characterized through FACS by staining for cTnT. The results for WT and the Het KO line are presented in Figure 19 and 20, respectively.

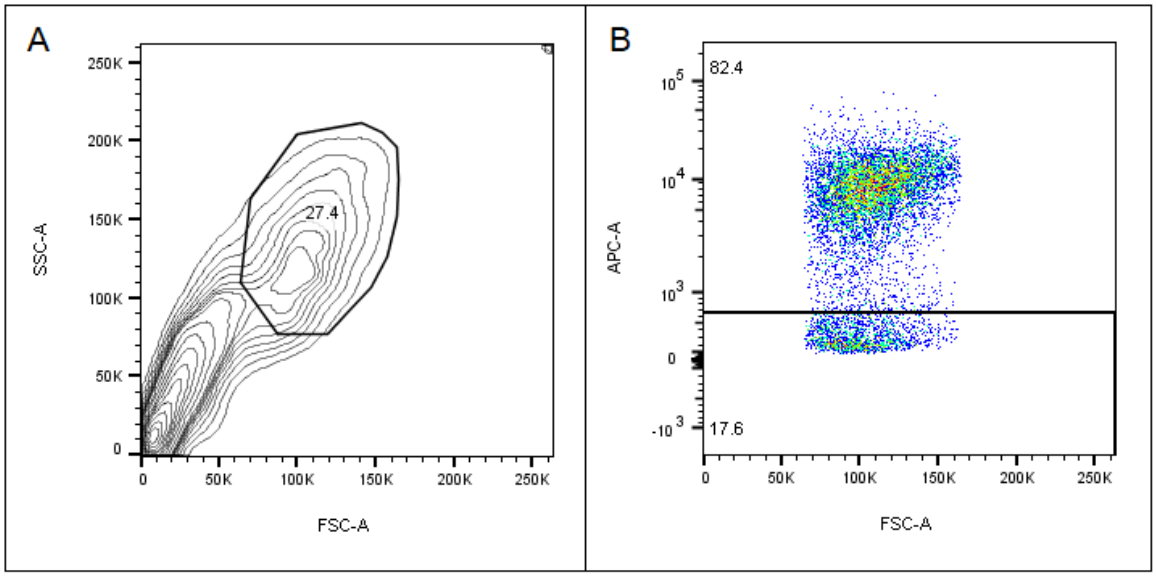

Figure 19. Characterization of WT iPSC-CMs by staining for cTnT and analysis through FACS. Panel A shows an initial gating of live cells from the total population. Panel B shows the gated cells plotted with forward scatter (FCS) against cTnT expression.

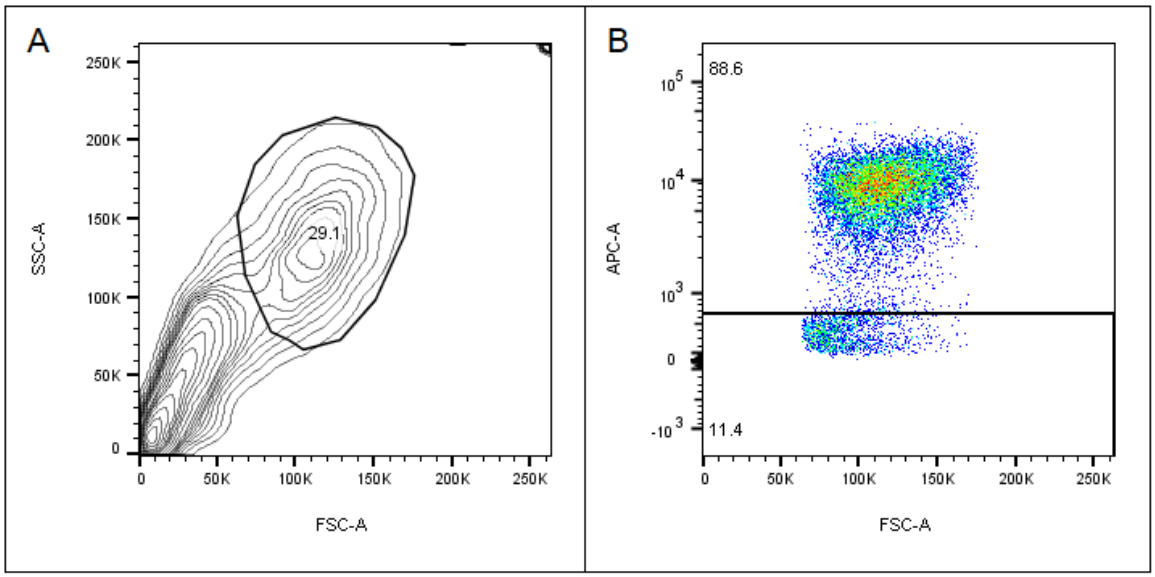

Figure 20. Characterization of Het KO iPSC-CMs by staining for cTnT and analysis through FACS. Panel A shows an initial gating of live cells from the total population. Panel B shows the gated cells plotted with forward scatter (FCS) against cTnT expression.

From Figure 19 and 20, it is shown that about 82% and 89% of the WT and Het KO population, respectively, stained positive for cTnT. The gate in panel B of Figure 19 and 20 was set based on the isotype control and validated with the unstained control to neglect any non-specific background staining or autofluorescence of the iPSC-CMs, see Appendix G.

The iPSC-CMs were further characterized by ICC by staining for cTnT as well as α-actinin, PLN and SERCA2. The results for WT and the Het KO iPSC-CMs are presented in Figure 21 and 22.

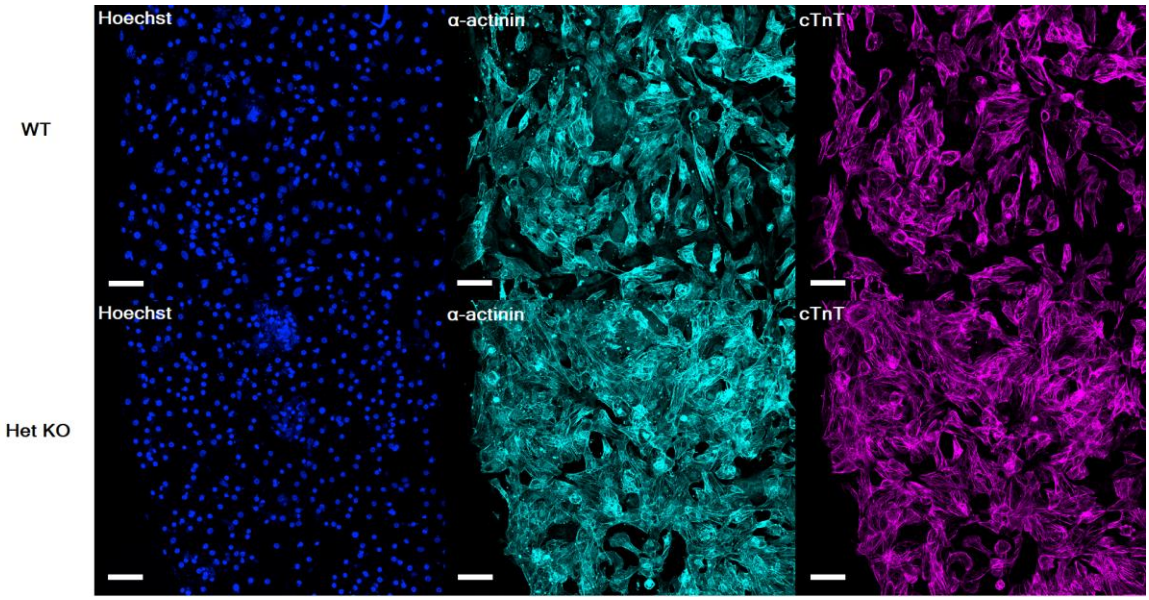

Figure 21. ICC images for WT (upper row) and the Het KO (lower row) iPSC-CMs from staining for cardiomyocyte markers. From left to right, DNA, i.e. cell nuclei, is visualized in blue, α-actinin in cyan and cTnT in magenta. The scalebar measures 100 µm.

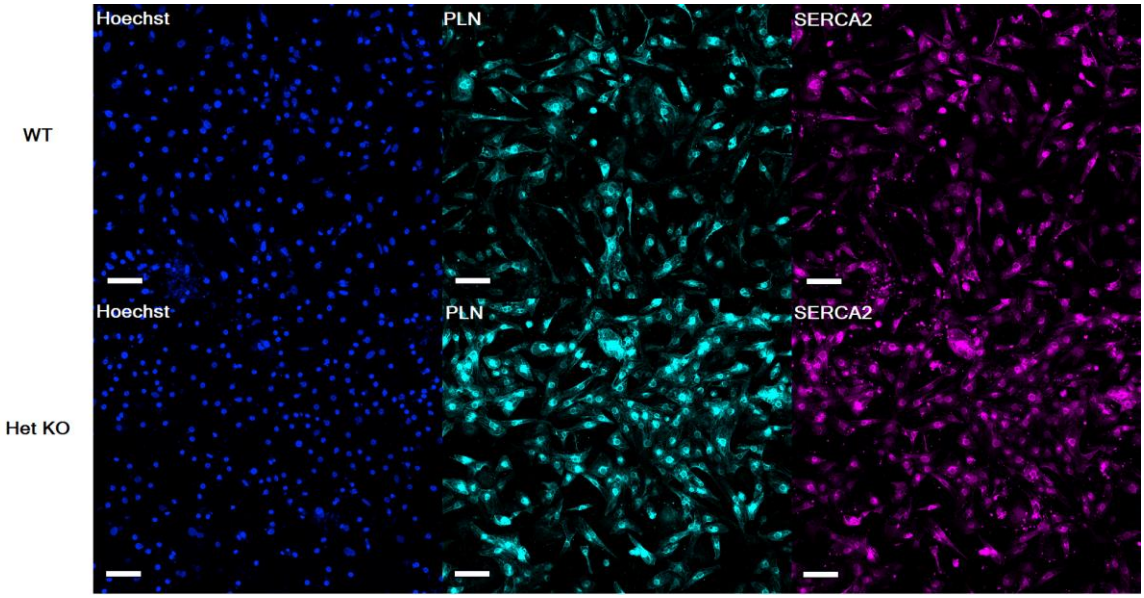

Figure 22. ICC images for WT (upper row) and the Het KO (lower row) iPSC-CMs from staining for cardiomyocyte markers. From left to right, DNA, i.e. cell nuclei, is visualized in blue, PLN in cyan and SERCA2 in magenta. The scalebar measures 100 µm.

As can be observed in Figure 21 and 22, the cardiomyocyte markers were found at the location of the cell colonies, as indicated by the Hoechst stain in blue. The specificity of the stains was validated by a negative control, see Appendix H. Both WT and Het KO iPSC-CMs stained positive for the cardiomyocyte markers in Figure 21 and 22. However, the stain appeared brighter in the Het KO iPSC-CMs compared to WT.

The protein expression of the iPSC-CMs was analyzed by Western blotting. The result is visualized in Figure 23.

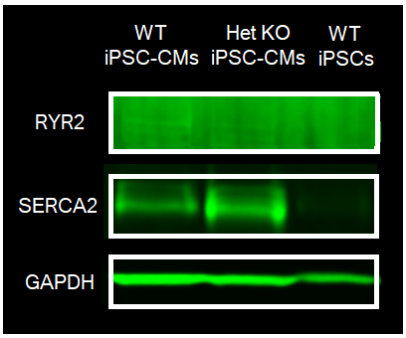

Figure 23. Western blot of WT and Het KO iPSC-CMs as well as WT iPSCs from day 0 of differentiation including RYR2, SERCA2 and GAPDH as the loading control.

From Figure 23, the WT and Het KO iPSC-CMs show equal amount of loaded protein based on the expression of GAPDH in the role of a loading control. The WT iPSCs show a slightly lower loading, but has no expression of either RYR2 or SERCA2. Both WT and Het KO iPSC-CMs express SERCA2, with a slightly higher expression in the Het KO sample. However, RYR2 has a higher expression in WT iPSC-CMs compared to the Het KO iPSC-CMs, suggesting a knock-down of the protein in the Het KO iPSC-CMs.

The impedance of the iPSC-CMs was measured to obtain data of beat rate and amplitude, a surrogate measure of contractility. Figure 24 shows an example of the trace of impedance measurement obtained from a well of WT iPSC-CMs. Wells for both WT and Het KO iPSC-CMs showed a similar trace.

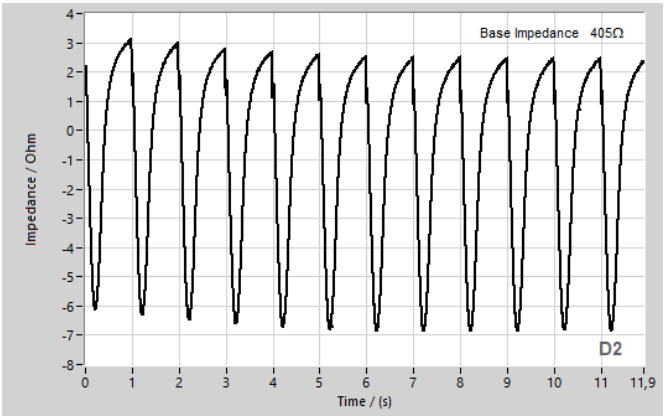

Figure 24. Impedance measurement from one well of WT iPSC-CMs recorded at pacing of 1 Hz.

From Figure 24, it can be observed that the iPSC-CMs showed a relatively regular impedance in terms of both beat rate and amplitude. The data of beat rate and amplitude from eight wells for both WT and Het KO iPSC-CMs was further analyzed. The result is presented in Figure 25.

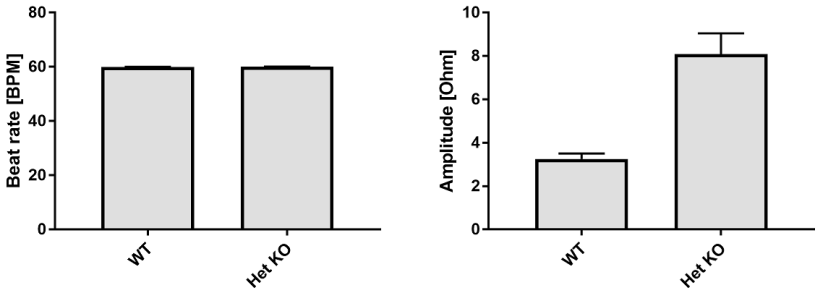

Figure 25. Mean ± SEM of beat rate and amplitude of WT and Het KO iPSC-CMs paced at 1 Hz. n=8.

As seen in Figure 25, both WT and Het KO iPSC-CMs were able to keep pace, with beat rates at 60 bpm corresponding to 1 Hz. The Het KO iPSC-CMs showed approximately a 2-fold increase in amplitude compared to WT.

5. Discussion and suggestions for future research

The results obtained in this thesis show promising results for generation of patient-centric *in vitro* cardiovascular models by gene modification of iPSCs and differentiation into cardiomyocytes. However, future work remains for both the SNP1 line and the Het KO line before the lines can act as models and be treated with drugs to detect differential pharmacology responses compared to WT. In this section, improvements to obtain the SNP1 line is discussed, as well as the required work before the SNP1 line can be used as an *in vitro* cardiovascular model. In addition, risk and ethics regarding the use of CRISPR/Cas9 is considered. For the Het KO line, differences between the Het KO line and WT are discussed as well as potential improvements to completely validate the knock-down of RYR2. The findings from this thesis are compared with results from other studies of RYR2 KO. At last, the potential of patient-centric *in vitro* cardiovascular models for drug testing is raised as an important improvement in drug discovery and development.

5.1. SNP1 line

From the reverse transfection of hiPSCs to obtain lines with the SNP1 mutation, 21 lines were obtained from transfection using 20 nM ssODNs. Out of these, 19 lines were considered positive from the Surveyor nuclease assay. In the case of transfection with 40 nM ssODNs, 19 out of 22 lines were considered positive. There was no significant difference in obtained lines between the two conditions, indicating that a concentration of 40 nM ssODNs was sufficiently low to not cause a toxic effect on the cells. Furthermore, there was only one line obtained with the desired SNP1 mutation, from a total of 43 lines. Based on the results from the Surveyor nuclease assay, which showed that a majority of the obtained cell lines had mutations, the transfection seemed to have succeeded in most of the cell lines. However, nearly all of them probably underwent the NHEJ pathway after Cas9 cleavage which resulted in indels instead of SNPs. This suggests that a higher concentration of ssODNs could result in additional lines with the desired mutation, by further promoting the HDR pathway after Cas9 cleavage, without reaching a toxic level. To obtain additional cell lines after transfection, there are improvements that can be considered to increase the survival of the single cells after sorting. These include decreasing the sorting time of the cells by optimizing the cell density of the starting cell suspension to improve the transfection efficiency, as well as maintaining ideal temperature conditions for the cells during transfer and sorting. Furthermore, a higher overall clonal efficiency has been observed with the use of Geltrex as the coating matrix and RevitaCell as the ROCK inhibitor, compared to DEF-CS COAT-1 and Y-27632, respectively, which were used in this thesis [29].

Line 40-11, with the potential SNP1 mutation, shows a promising outcome from sequencing with both forward and reverse primers giving a consistent result of the desired SNP, as presented in Figure 10 and 11, respectively. Furthermore, there are two peaks present at the mutation site in the chromatograms, one for the desired SNP and the other conserving the WT sequence, suggesting that a heterozygous SNP was obtained. As seen in Figure 12, the off-target analysis showed no evidence of any off-target events. However, Sanger sequencing is limited to sequencing of specific regions of the genome, giving the possibility that other regions of the genome could be affected. Consequently, the next step for complete validation of the heterozygous SNP1 mutation of line 40-11 is sequencing of the whole

genome using Next Generation Sequencing (NGS). NGS of the WT hiPSCs is essential to include for detection of mutations present in the line before transfection, as in the case of the *KBTBD6* gene visualized in Figure 12. In addition, the result from NGS can be used to validate that the detected SNPs in line 40-11 are heterozygous mutations. Hence, this is required to be able to conclude that an iPSC line has been obtained with the desired heterozygous SNP1 mutation. Thereafter, this line can be characterized to validate the genomic stability and pluripotency before differentiation, and then differentiation into cardiomyocytes can be initiated. The same procedure carried out for the Het KO line should be performed for the SNP1 line after cardiomyocyte differentiation to detect any differences in its characteristics, including evaluation of cardiomyocyte markers, protein expression and measurement of beat rate and amplitude.

Although CRISPR/Cas9 has shown to be a promising tool in gene editing by being faster, cheaper and more precise compared to other gene editing methods, there are risks in using it for more permanent applications. One of the risks with CRISPR/Cas9 is the potential off-target activity that has been investigated in this thesis. In this case, no indications of off-target events were detected. However, as mentioned previously, the whole genome needs to be sequenced and screened for potential mutations, other than the desired SNP, to be able to completely reject the possibility. Additionally, another risk is the efficiency of CRISPR/Cas9. From this thesis, one out of 43 lines obtained the desired mutation which corresponds to approximately 2%. Consequently, there is a low chance to obtain the desired mutation during CRISPR/Cas9 transfection. However, several other types of mutations will be incorporated, as indicated from the number of positive lines obtained from the Surveyor nuclease assay and the subsequent sequencing of these lines. This is mainly due to the high efficiency of indel generation via the NHEJ pathway, compared to the low efficiency of the HDR pathway, which proposes a high risk of unwanted adverse effects.

Despite the risks of CRISPR/Cas9, it has been used for gene editing of embryos and germ cells. There are several studies in a range of animal models that have shown successful results. One study of particular interest is the correction of a genetic disease, causing cataract development, in mice. The correction was successful in that the resulting mice could transmit the correction to their off-spring and thereby prevent the on-set of the genetic disorder [30]. Furthermore, CRISPR/Cas9 has been applied to human tripronuclear zygotes as an attempt to edit the *HBB* gene, which resulted in low efficiency and mosaic embryos with several off-target events detected [31]. These findings indicate that further research is required before introducing CRISPR/Cas9 in clinical applications. If CRISPR/Cas9 becomes a reliable gene editing tool in the future, the prevailing discussions regarding ethical aspects need to be considered. The correction of non-medical conditions is a topic that is highly debated. This includes gene editing to obtain more desirable traits, such as physical characteristics, including specific hair and eye colors, and athletic or aesthetic talents. From a scientific perspective, this would be complex, since these traits are polygenic and dependent of regulatory sequences and epigenetics [32]. From an ethical perspective, this would be difficult as well. One of the reasons is that gene editing would possibly become a tool that is available only for privileged people. This would further increase the gap between rich and poor. Furthermore, questions of consent are raised, considering whether it is ethically acceptable to make changes to an embryo without the consent of the person it would develop into. Another concern is the potential danger this could imply for future generations, if the gene modifications have unexpected adverse effects. Regardless of the future ethical concerns of CRISPR/Cas9, it remains a valuable tool to cure many genetic diseases which are currently incurable. This weighs as a strong argument to keep pursuing research within this field.

5.2. Het KO line

Since the procedure for characterization and differentiation of the Het KO line was carried out for a WT line in parallel, it could be observed that the Het KO line had similar characteristics as the WT before differentiation. Both had a normal male karyotype of 23 chromosomes, as presented in Figure 13 and 14, and the high degree of pluripotency was nearly identical as indicated by FACS in Figure 15 and 16 as well as ICC in Figure 17 and 18. Despite their similarities before differentiation, differentiation of the Het KO line resulted in a purer cardiomyocyte population compared to WT. This could be seen visually in the microscope during differentiation, but was validated after differentiation by FACS and ICC. From cTnT staining and analysis through FACS, about 89% of the Het KO population stained positive compared to 82% of the WT population. The result could be further validated through FACS by staining for other cardiomyocyte markers. However, analysis using ICC, showed that three other cardiomyocyte markers, in addition to cTnT, showed an increased expression in the Het KO line, confirming the quantitative result from FACS, see Figure 21 and 22. The expression of SERCA2 from Western blotting further confirms this result, see Figure 23, since the Het KO line expressed a higher level of SERCA2 with the same amount of protein added, as indicated by GAPDH in the role of loading control. This result is consistent with two additional KO lines that has been evaluated in the project that this thesis is part of. However, the difference in cardiomyocyte differentiation of RYR2 KO cells has not been observed in embryonic stem (ES) cell-derived cells, neither in terms of cellular morphology nor differentiation profile [33]. The use of different differentiation protocols could be a possible reason to the inconsistency of the results. These findings indicate that further research is required to detect other potential effects of RYR2 KO.

The protein expression of the iPSC-CMs was further analyzed by Western blotting to validate the knock-down of the RYR2 protein. As seen in Figure 23, there was high background levels. However, the light indications of bands suggest that there is a decreased expression of RYR2 in the Het KO line. Before drawing a conclusion regarding this, the Western blotting needs to be repeated. Potential improvements could include shorter storage between cell harvest and analysis, change of blocking buffer, decreased dilution and/or change of antibody. A shorter storage time could prevent any potential degradation of the protein. The high background levels could be caused by low efficiency of the blocking buffer. However, all the analyzed proteins originate from the same blot which was treated with the same blocking buffer. In the case for SERCA2 and GAPDH, the blots showed pure staining of the bands. This indicates that the high background levels might have been caused by non-specific binding by the RYR2 antibody. If this is the case, the background levels would be even higher with a decreased dilution of the antibody. Therefore, a reasonable solution would be to use another RYR2 antibody.

The functional measurements of the iPSC-CMs, visualized in Figure 25, showed that both WT and the Het KO line kept the pace of 60 bpm, corresponding to 1 Hz. The Het KO line showed a 2-fold increase in amplitude compared to WT. In addition, the two other existing Het KO lines in the project have shown the same pattern. Based on the hypothesis that RYR2 has a reduced expression in the Het KO line, the increase in amplitude could be caused by an increased contractile force of the myofilaments in the cardiomyocytes to compensate for the decreased concentration of cytosolic Ca^{2+} available with a less active RYR2. A study of mice with 50% depletion of RYR2 has shown a slight decrease of the amplitude of cytosolic and mitochondrial Ca^{2+} signaling which could indicate that the communication between the organelles is disrupted by RYR2 reduction [34]. A next step in

the project would be to characterize the Ca^{2+} signaling by examining the Ca^{2+} content differences between WT and Het KO iPSC-CMs. This can be done by caffeine application to the cells. Caffeine is a RYR opener which would cause complete SR Ca^{2+} release into the cytosol. Consequently, the amplitude of Ca^{2+} transient would be a measure of the SR Ca^{2+} content. Furthermore, SERCA2 activity is disrupted during caffeine application, making the time constant of Ca^{2+} decay a measure of NCX activity as Ca^{2+} removal would mainly be carried out by the NCX [35].

5.3. Patient-centric *in vitro* cardiovascular models for use in drug testing

An alternative to establish patient-centric *in vitro* cardiovascular models is to obtain biopsies from patients with cardiac diseases. These biopsies can be used to generate iPSCs with the genetic disorder of the patients which can be differentiated into cardiomyocytes. A study has been carried out in which skin biopsies of a patient with CPVT1 was taken to generate iPSCs. By differentiation of the iPSCs into cardiomyocytes, the cardiomyocytes were shown to sustain CPVT1 characteristics, including the Ca^{2+} signaling phenotype [36]. Another study used iPSC-CMs from patients diagnosed with CPVT2 for evaluation of drug response. The study included several drugs for treatment of CPVT2, including flecainide and labetalol. Flecainide was observed to be effective for suppression of arrhythmogenic activity, whereas labetalol was shown to be ineffective. The *in vitro* results were consistent with the clinical results of the patient. This proposes patient-centric *in vitro* modeling as a feasible tool for predicting pharmacological clinical responses [37]. A limitation of using patient-derived cells for disease modeling is the potential presence of other mutations in the genome that might cause unexpected effects, independent of the mutation causing the cardiac disease in consideration. Consequently, it is important to include controls to obtain a reliable result. On the contrary, this limitation can be beneficial for the donor patient, since the results would reflect the response in the patient with a higher specificity.

6. Conclusion

From this thesis, one hiPSC line with a potential heterozygous SNP1 mutation has been obtained. Based on results from Sanger sequencing, the hiPSC line seemed to have obtained the SNP1 mutation in one allele, while conserving the WT sequence in the other allele. In addition, no evidence of off-target activity by the gRNA from CRISPR/Cas9 transfection was detected. However, NGS is required to fully validate this finding and to reject the possibility of other mutations obtained during transfection. Furthermore, the Het KO line has shown a functional behavior as a cardiovascular model, although the RYR2 knockdown needs to be fully validated by repeating Western blotting, before the Het KO line can act as a cardiovascular model of reduced RYR2 expression. The SNP1 line needs to undergo the same procedure as the Het KO line for characterization of the iPSC-CMs. Once both hiPSC lines have been fully characterized, they will be able to act as *in vitro* cardiovascular safety models with genetic variability in calcium handling and differential pharmacology responses can be measured by treating the differentiated iPSC-CMs with drugs. Since the Het KO iPSC-CMs show an increased contractility amplitude compared to WT without drug treatment, there is a high probability that there is a differential drug response as well. The future research within patient-centric *in vitro* cardiovascular models, including the remaining work within this project, will help improve and make human *in vitro* models more realistic by mimicking existing mutations within the population. This is key to providing safe and efficacious drugs for the entire population.

7. References

1. Minotti G. Cardiotoxicity of non-cardiovascular drugs. New York: John Wiley & Sons; 2010.
2. Varga Z V, Ferdinandy P, Liaudet L, Pacher P. Drug-induced mitochondrial dysfunction and cardiotoxicity. Am J Physiol Heart Circ Physiol. 2015;309(9):H1453-67.
3. Morgan P, Brown DG, Lennard S, Anderton MJ, Barrett JC, Eriksson U, et al. Impact of a five-dimensional framework on R&D productivity at AstraZeneca. Nat Rev Drug Discov. 2018;17(3):167–81.
4. Zhang X-H, Morad M. Calcium signaling in human stem cell-derived cardiomyocytes: Evidence from normal subjects and CPVT afflicted patients. Cell Calcium. 2016;59(2–3):98–107.
5. Milting H, Lukas N, Klauke B, Körfer R, Perrot A, Osterziel K-J, et al. Composite polymorphisms in the ryanodine receptor 2 gene associated with arrhythmogenic right ventricular cardiomyopathy. Cardiovasc Res. 2006;71(3):496–505.
6. Ran Y, Chen J, Li N, Zhang W, Feng L, Wang R, et al. Common RyR2 variants associate with ventricular arrhythmias and sudden cardiac death in chronic heart failure. Clin Sci (Lond). 2010;119(5):215–23.
7. Crossman DJ, Ruygrok PR, Soeller C, Cannell MB, Cannell MB. Changes in the Organization of Excitation-Contraction Coupling Structures in Failing Human Heart. Schwartz A, editor. PLoS One. 2011;6(3):e17901.
8. Kandilci HB, Tuncay E, Zeydanli EN, Sozmen NN, Turan B. Age-related regulation of excitation-contraction coupling in rat heart. J Physiol Biochem. 2011;67(3):317–30.
9. Bidasee KR, Dinçer UD, Besch HR. Ryanodine receptor dysfunction in hearts of streptozotocin-induced diabetic rats. Mol Pharmacol. 2001;60(6):1356–64.
10. Milnes JT, MacLeod KT. Reduced ryanodine receptor to dihydropyridine receptor ratio may underlie slowed contraction in a rabbit model of left ventricular cardiac hypertrophy. J Mol Cell Cardiol. 2001;33(3):473–85.
11. Matsui H, MacLennan DH, Alpert NR, Periasamy M. Sarcoplasmic reticulum gene expression in pressure overload-induced cardiac hypertrophy in rabbit. Am J Physiol. 1995;268(1):C252-8.
12. Marieb EN HK. Human anatomy & physiology. 9th ed. Pearson Education, Inc. Harlow: Pearson Education Limited; 2015.
13. Kumari N, Gaur H, Bhargava A. Cardiac voltage gated calcium channels and their regulation by β-adrenergic signaling. Life Sci. 2018;194:139–49.
14. Zamponi GW, Striessnig J, Koschak A, Dolphin AC. The Physiology, Pathology, and Pharmacology of Voltage-Gated Calcium Channels and Their Future Therapeutic Potential. Pharmacol Rev. 2015;67(4):821–70.
15. Bround MJ, Asghari P, Wambolt RB, Bohunek L, Smits C, Philit M, et al. Cardiac ryanodine receptors control heart rate and rhythmicity in adult mice. Cardiovasc Res. 2012;96(3):372–80.
16. Van Petegem F. Ryanodine Receptors: Structure and Function. J Biol Chem. 2012;287(38):31624–32.
17. Medeiros-Domingo A, Bhuiyan ZA, Tester DJ, Hofman N, Bikker H, van Tintelen JP, et al. The RYR2-Encoded Ryanodine Receptor/Calcium Release Channel in Patients Diagnosed Previously With Either Catecholaminergic Polymorphic Ventricular Tachycardia or Genotype Negative, Exercise-Induced Long QT Syndrome. J Am Coll Cardiol. 2009;54(22):2065–74.

18. Lian X, Hsiao C, Wilson G, Zhu K, Hazeltine LB, Azarin SM, et al. Robust cardiomyocyte differentiation from human pluripotent stem cells via temporal modulation of canonical Wnt signaling. Proc Natl Acad Sci. 2012;109(27):E1848–57.
19. Hsu PD, Lander ES, Zhang F. Development and applications of CRISPR-Cas9 for genome engineering. Cell. 2014;157(6):1262–78.
20. Sander JD, Joung JK. CRISPR-Cas systems for editing, regulating and targeting genomes. Nat Biotechnol. 2014;32(4):347–55.
21. Paquet D, Kwart D, Chen A, Sproul A, Jacob S, Teo S, et al. Efficient introduction of specific homozygous and heterozygous mutations using CRISPR/Cas9. Nature. 2016;533(7601):125–9.
22. Kwart D, Paquet D, Teo S, Tessier-Lavigne M. Precise and efficient scarless genome editing in stem cells using CORRECT. Nat Protoc. 2017;12(2):329–54.
23. Salsman J, Dellaire G. Precision genome editing in the CRISPR era. Biochem Cell Biol. 2017;95(2):187–201.
24. Galbraith DW, Anderson MT, Herzenberg LA. Flow cytometric analysis and FACS sorting of cells based on GFP accumulation. Methods Cell Biol. 1999;58:315–41.
25. Alberts B, Wilson J, Hunt T. Molecular biology of the cell. 5th ed. New York: Garland Science; 2008.
26. Qiu P, Shandilya H, D'Alessio JM, O'Connor K, Durocher J, Gerard GF. Mutation detection using SurveyorTM nuclease. Biotechniques. 2004;36(4):702–7.
27. Wang X. Next-Generation Sequencing Data Analysis. 1st ed. Boca Raton: CRC Press; 2016.
28. Burry RW. Immunocytochemistry. New York: Springer New York; 2010.
29. Chen Y-H, Pruett-Miller SM. Improving single-cell cloning workflow for gene editing in human pluripotent stem cells. Stem Cell Res. 2018;31:186–92.
30. Wu Y, Liang D, Wang Y, Bai M, Tang W, Bao S, et al. Correction of a Genetic Disease in Mouse via Use of CRISPR-Cas9. Cell Stem Cell. 2013;13(6):659–62.
31. Liang P, Xu Y, Zhang X, Ding C, Huang R, Zhang Z, et al. CRISPR/Cas9-mediated gene editing in human tripronuclear zygotes. Protein Cell. 2015;6(5):363–72.
32. Vassena R, Heindryckx B, Peco R, Pennings G, Raya A, Sermon K, et al. Genome engineering through CRISPR/Cas9 technology in the human germline and pluripotent stem cells. Hum Reprod Update. 2016;22(4):411–9.
33. Yang H-T, Tweedie D, Wang S, Guia A, Vinogradova T, Bogdanov K, et al. The ryanodine receptor modulates the spontaneous beating rate of cardiomyocytes during development. Proc Natl Acad Sci U S A. 2002;99(14):9225–30.
34. Bround MJ, Wambolt R, Cen H, Asghari P, Albu RF, Han J, et al. Cardiac Ryanodine Receptor (Ryr2)-mediated Calcium Signals Specifically Promote Glucose Oxidation via Pyruvate Dehydrogenase. J Biol Chem. 2016;291(45):23490–505.
35. Morse JC, Huang J, Khona N, Miller EJ, Siwik DA, Colucci WS, et al. Up-regulation of Intracellular Calcium Handling Underlies the Recovery of Endotoxemic Cardiomyopathy in Mice. Anesthesiology. 2017;126(6):1125–38.
36. Fatima A, Xu G, Shao K, Papadopoulos S, Lehmann M, Arnáiz-Cot JJ, et al. In vitro Modeling of Ryanodine Receptor 2 Dysfunction Using Human Induced Pluripotent Stem Cells. Cell Physiol Biochem. 2011;28(4):579–92.
37. Maizels L, Huber I, Arbel G, Tijsen AJ, Gepstein A, Khoury A, et al. Patient-Specific Drug Screening Using a Human Induced Pluripotent Stem Cell Model of Catecholaminergic Polymorphic Ventricular Tachycardia Type 2. Circ Arrhythmia Electrophysiol. 2017;10(6).

Appendix A: Sequences of SNP1 guideRNA, ssODNs and primers

In this appendix, the SNP1 sequence is presented together with sequences of the guideRNA, ssODNs, forward and reverse primers. The following sequence is the sequence surrounding SNP1.

CCTCAGCACCTCCCTCAGGCCACGGATGCAGTTTTCCTCCCCCAGTTTTGTAAGCA
TTAGTAATGAATGTTACCAGTACAGTCCAGAGTTCCCACTGGACATCCTCAAGTCC
AAAACCATACAGATGCTGACAGAAGCTGTTAAAGAGGGCAGTCTTCATGCCCGGG
ACCCAGTTGGAGGGACTACTGAATTCCTCTTTGTACCTCTCATCAAGCTTTTCTATA
CCCTGCTGATCATGGGCATCTTTCACAACGAGGACTTGAAGCACATCTTGCAGTTG
ATTGAGCCCAGTGTGTTTAAAGAAGCTGCCACTCCGGAGGAGGAGAGTGACACGC
TGGAGAAAGAGCTCAGTGTGGACGATGCAAAGCTGCAAGGAGCTGGTGAGGAAG
AAGCAAAGGGGAGCAAGCGGCCCAAGGAAGGCCTGCTCCAAATGAAACTGCCA
GAGCCAGTTAAATTGCAGGTAATCAGAACAAGAGACTTGAGTGAATTTCAGAATT
GCTAAGCATTAAGGTATTAGAACATGCCTTTGTTTCTTTCTCTGTGTGTGTGTTTATT
TCTTTGCATTCCTGTGTAATGGTAGTTCTTCATAAAATTAACTAACTTCCTATTCTTT
TCCCTCTTATTCATTAGCCATCTCCTCTTGTTTCCCAGATGCTTTTTACCTTCATTAC
ATTGGAATACCTGAAATACAAGCCATCAAATACCCCTTTCCACCCATATTTCCACTC
TTACCAACCTTAGAATACTTGTTTACCAGTAGATGCACCCATTGTCACATAGCAAGG
TTTTACTTTCCCCTAGTA

The SNP1 forward and reverse primers are marked in yellow. The underlined sequence indicates the SNP1 ssODN, including the site-specific sequence changes marked in red. The PAM site, CCA>CAA, is marked in green and SNP1, GGC>AGC, is marked in blue. The WT ssODN differs from the SNP1 ssODN by the exclusion of the SNP1 mutation. The binding site of the guideRNA is marked in bold. The sequence of the guideRNA is presented below.

CTTGGGCCGCTTGCCCCCCT TGG

Appendix B: Volumes of reagents used for cell passaging

In this appendix, the volumes of reagents used for cell passaging are presented for each plate size with the corresponding surface area, see Table B.1.

Table B.1. Volumes of reagents used for passaging cells according to plate size with corresponding surface area.

	Surface area	**Culture media**	**DEF-CS COAT-1 (1:10 dilution)**	**TrypLE Select**
384 well	0.056 cm^2	40 µL	25 µL	20 µL
96 well	0.32 cm^2	200 µl	35 µl	40 µl
48 well	1.0 cm^2	500 µl	200 µl	100 µl
24 well	1.9 cm^2	1.5 mL	300 µl	200 µl
12 well	3.9 cm^2	2 mL	500 µl	400 µl

Appendix C: Sequences of off-target genes and primers

In this appendix, the sequences of the potential off-target regions and their forward and reverse primers are presented, see Table C.1.

Table C.1. Sequences of potential off-target regions, including forward and reverse primers used for PCR amplification and sequencing. The PAM sites are indicated in bold and the mismatches of the target sequence are indicated by lowercase letters.

Gene	Target	Strand	Forward primer	Reverse primer
CHRFAM7A	CTTGGGCatCTTGCCCCCgT**CGG**	+	CCAGCCTGGGTGACATAGTG	GACTGACAAGTCGGCCAGAG
CHRNA7	CTTGGGCatCTTGCCCCCgT**CGG**	-	GACTGACAAGTCGGCCAGAG	CCAGCCTGGGTGACATAGTG
PLEC	CTTGcGCCGCacGCCCtCCT**CGG**	+	CTCTGAGCTGACACCTTCCG	CCTGCAGCAAAGCTTCCTCT
KBTBD6	CTTGGGCCGCTTcCCaCCac**GGG**	+	CTCTCGTACATGCCACCTGT	GTCAGCGAGGGAAGGTTGAG

Appendix D: Chromatogram of sequences of line 40-11

In this appendix, the chromatograms of forward and reverse sequences of line 40-11 are presented, see Figure D.1 and D.2, respectively.

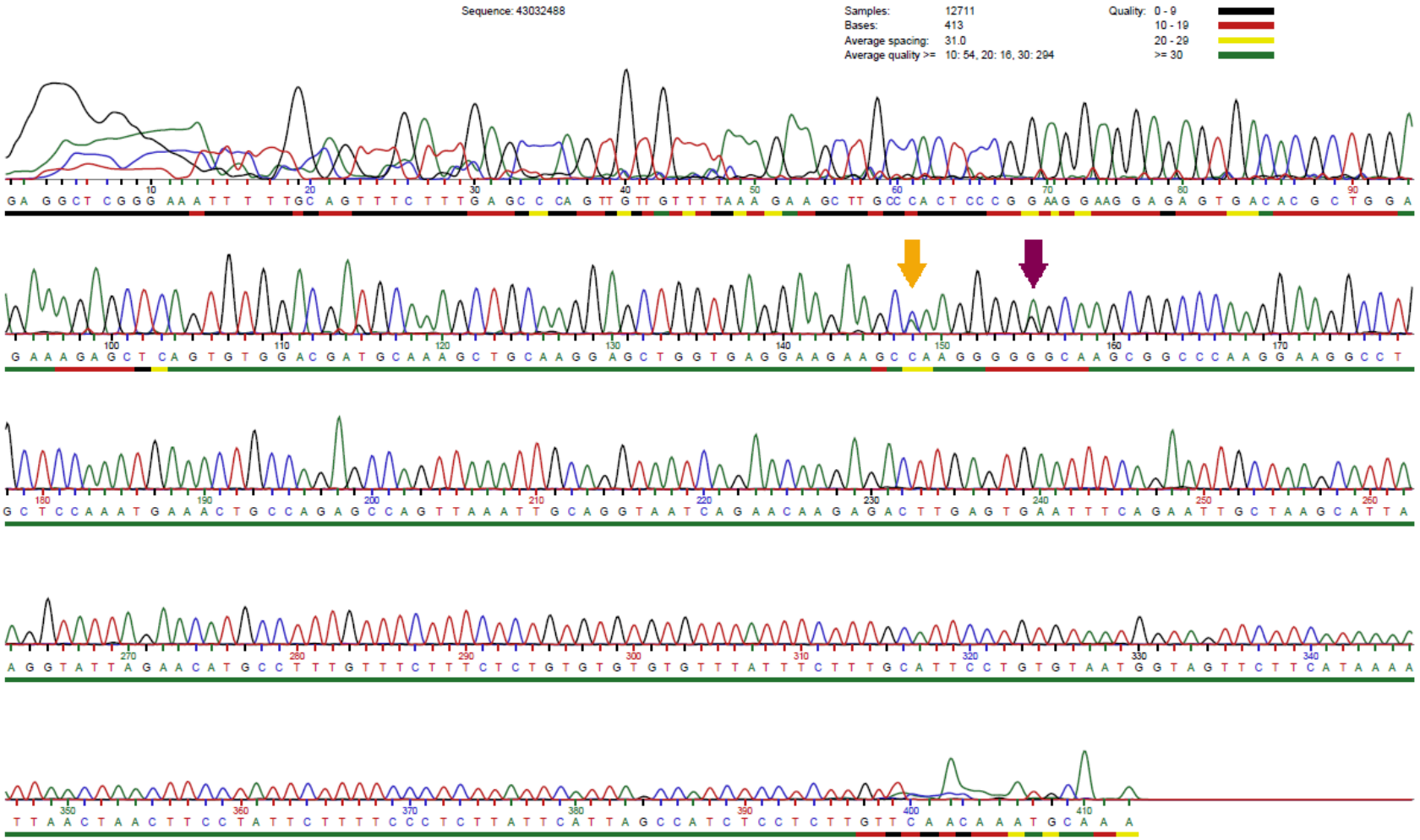

Figure D.1. Chromatogram of forward sequence of line 40-11. The silent mutation of the PAM site is indicated by the orange arrow. The desired SNP1 mutation is indicated by the purple arrow.

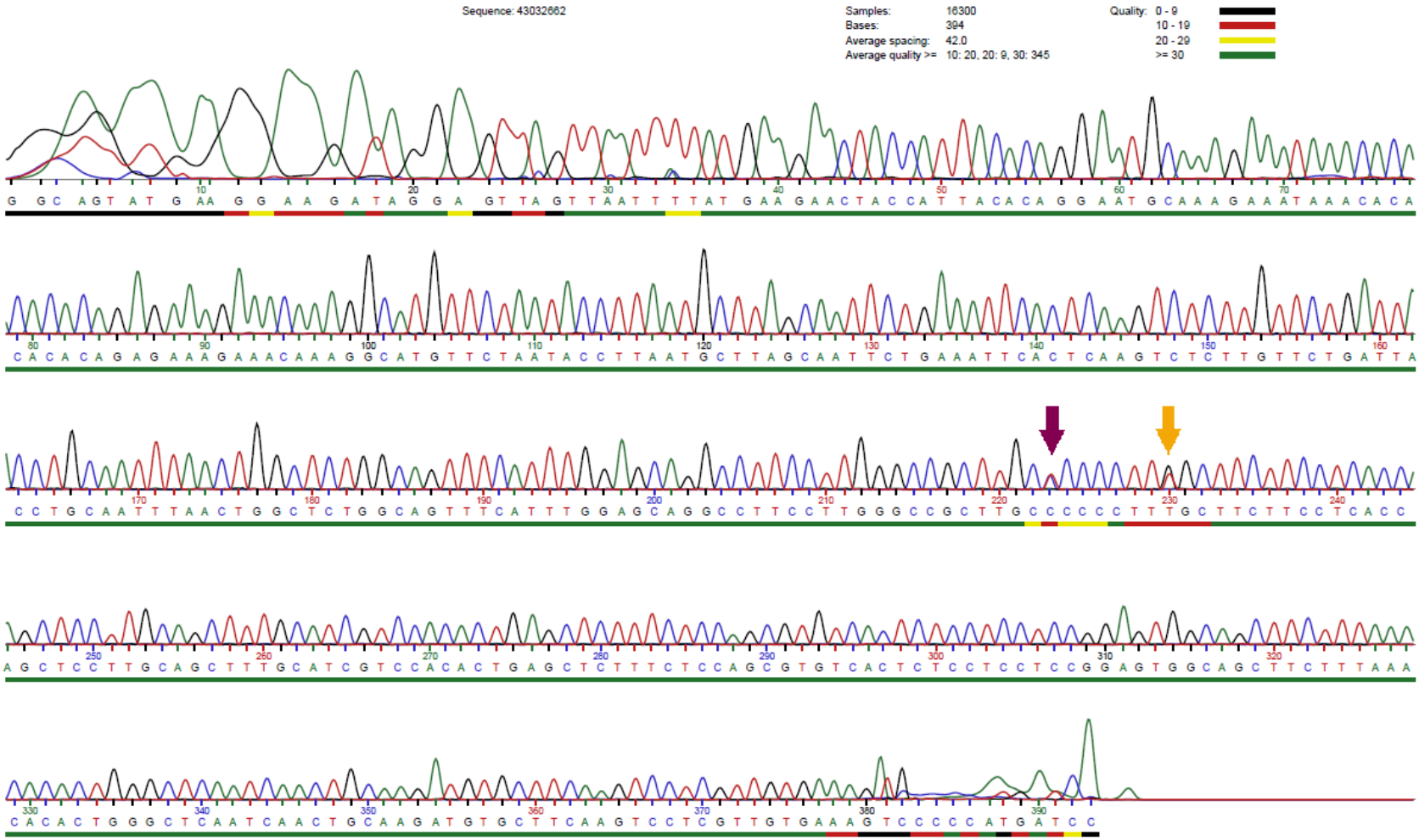

Figure D.2. Chromatogram of reverse sequence of line 40-11. The silent mutation of the PAM site is indicated by the orange arrow. The desired SNP1 mutation is indicated by the purple arrow.

Appendix E: FACS results for isotype control and unstained control for validation of pluripotency of iPSCs

In this appendix, the results from FACS analysis for validation of pluripotency of the iPSCs are presented for isotype control and unstained control.

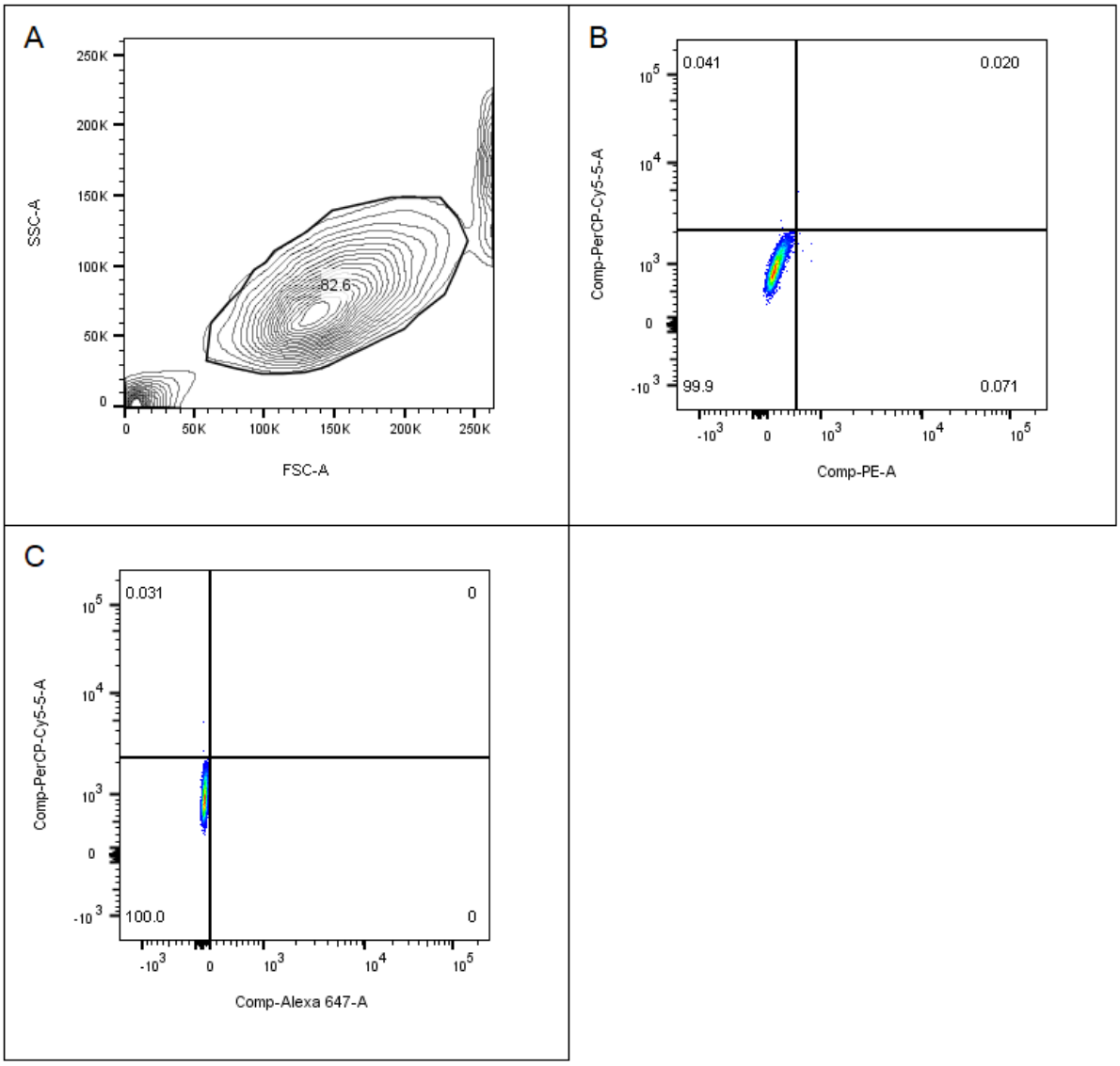

Figure E.1. Results from FACS analysis for validation of pluripotency for isotype control. Panel A shows an initial gating of live cells from the total population. In panel B and C, the gated cells are visualized in terms of SSEA-1 and Oct3/4 expression, and SSEA-4 and Oct3/4 expression, respectively.

The isotype control was stained with non-specific antibodies conjugated to the same fluorochrome as the specific antibodies to identify any non-specific background staining. The cells gated from panel A in Figure E.1. should therefore appear negative for all the stains. Consequently, the gates in panel B and C in Figure E.1 were set accordingly.

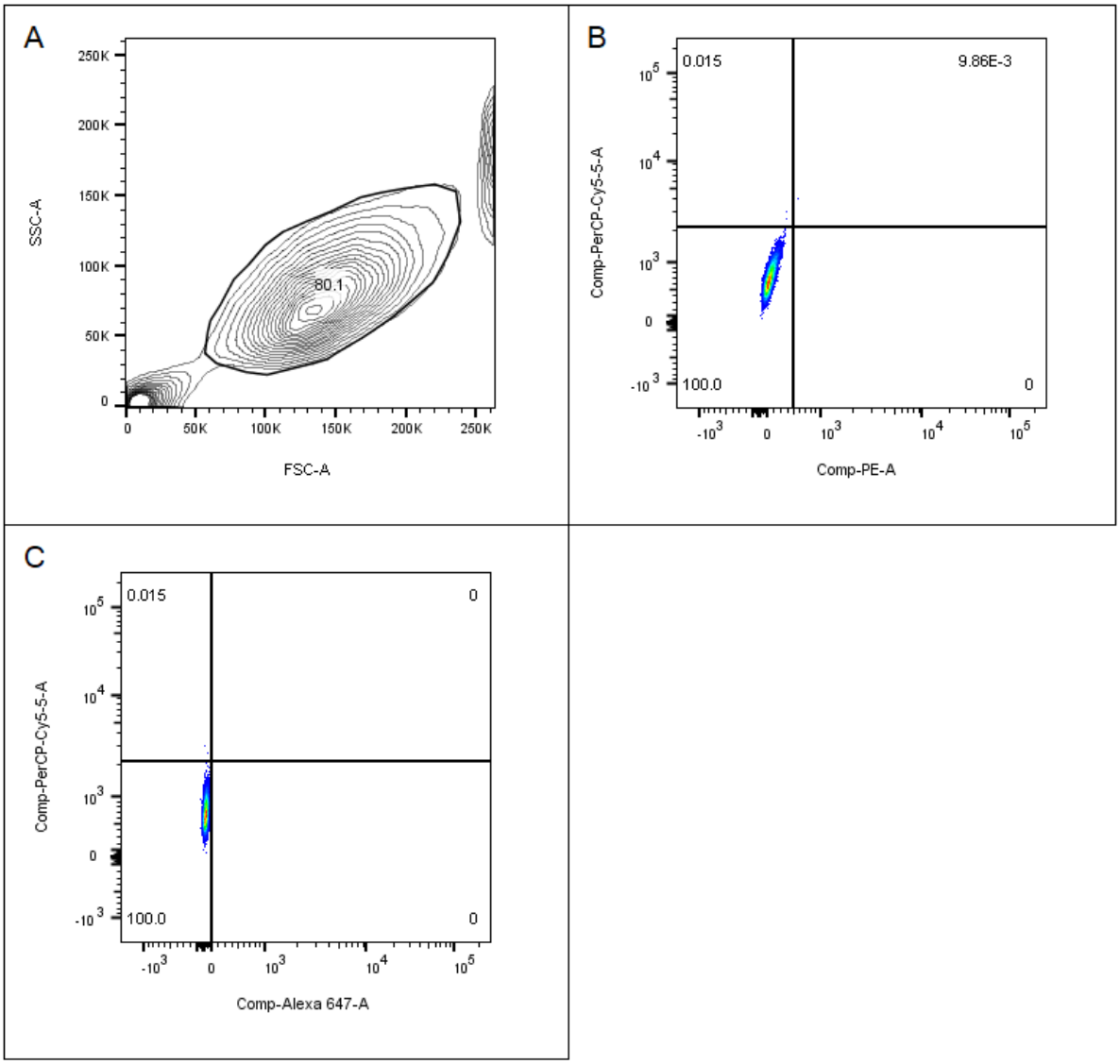

Figure E.2. Results from FACS analysis for validation of pluripotency for unstained control. Panel A shows an initial gating of live cells from the total population. In panel B and C, the gated cells are visualized in terms of SSEA-1 and Oct3/4 expression, and SSEA-4 and Oct3/4 expression, respectively.

The unstained control was used to identify any autofluorescence of the iPSCs. The sample was therefore not stained with any of the stains. The gates in panel B and C in Figure E.2 was set according to the isotype control which resulted in 100% of the population staining negative for all the stains. From these results, the set gates were concluded to be appropriate to use to determine the pluripotency of WT and Het KO iPSCs.

Appendix F: ICC results for negative control for validation of pluripotency of iPSCs

In this appendix, the results for the negative control validation of pluripotency of iPSCs by ICC is presented. The negative control was only stained with Hoechst stain and secondary antibodies, without any primary antibodies. The result is visualized in Figure F.1.

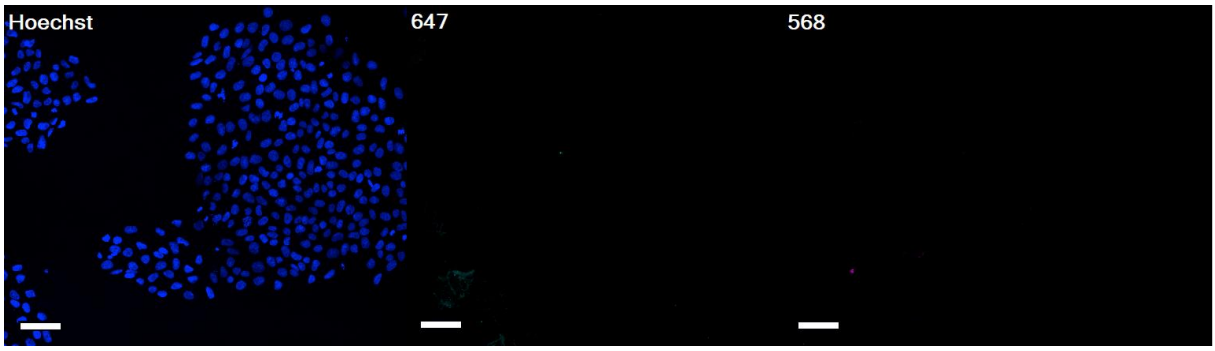

Figure F.1. Negative control for validation of pluripotency of iPSCs by ICC. From left to right, the Hoechst stain is visualized in blue, Alexa Fluor 647 Goat anti-Mouse in cyan and Alexa Fluor 568 Goat anti-Rabbit in magenta. The scalebar measures 100 µm.

As seen in Figure F.1. the secondary antibodies are not visualized in the absence of primary antibodies which confirms that the iPSCs are not autofluorescent.

Appendix G: FACS results for isotype control and unstained control for characterization of iPSC-CMs

In this appendix, the results from FACS analysis for characterization of the iPSC-CMs are presented for isotype control and unstained control.

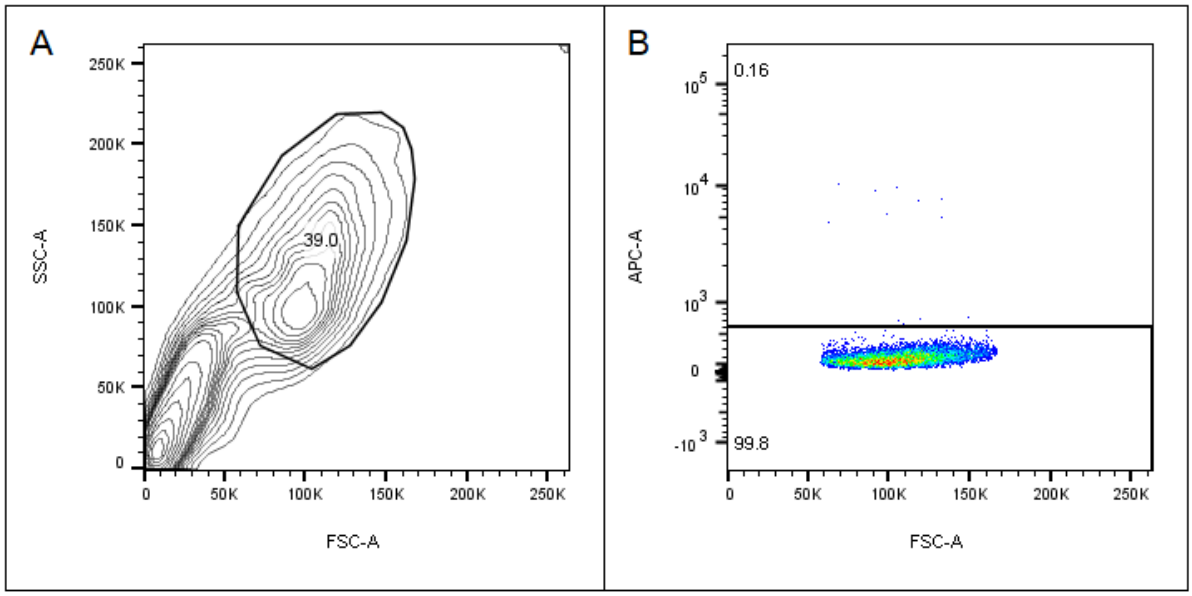

Figure G.1. Results from FACS analysis for characterization of iPSC-CMs for isotype control. Panel A shows an initial gating of live cells from the total population. Panel B shows the gated cells plotted with forward scatter (FCS) against troponin T expression.

The isotype control was stained with a non-specific antibody conjugated to APC, which was the same fluorochrome conjugated with the anti-cardiac troponin T antibody, to identify any non-specific background staining. The cells gated from panel A in Figure G.1. should therefore appear negative for APC in panel B. The gate in panel B in Figure G.1 were therefore set accordingly.

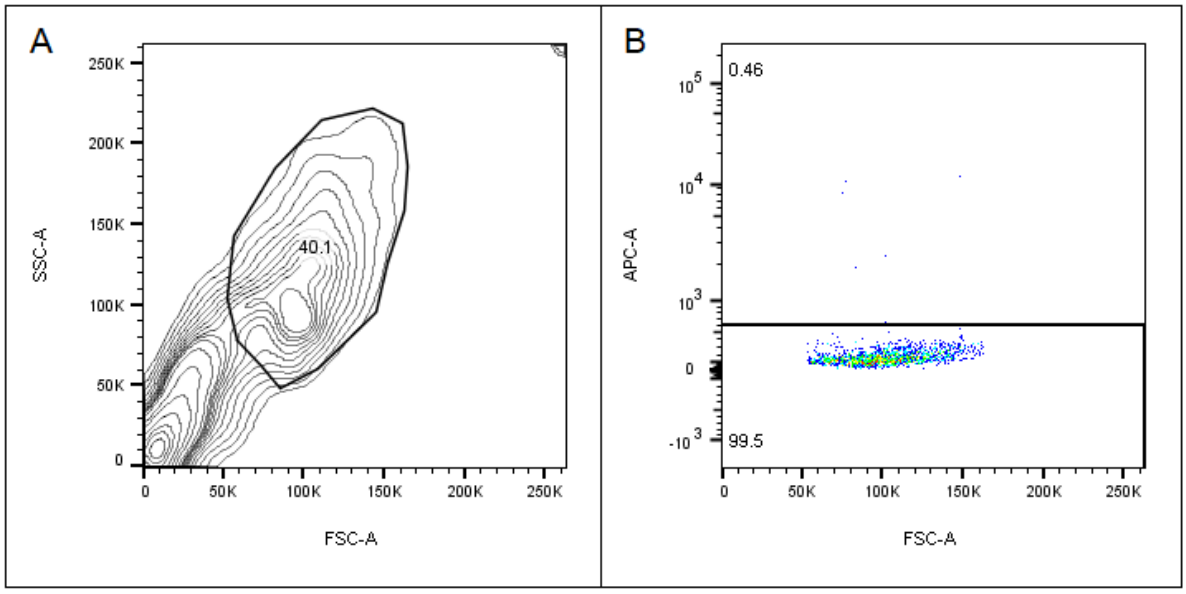

Figure G.2. Results from FACS analysis for characterization of iPSC-CMs for unstained control. Panel A shows an initial gating of live cells from the total population. Panel B shows the gated cells plotted with forward scatter (FCS) against troponin T expression.

The unstained control was used to identify any autofluorescence of the iPSC-CMs. The sample was therefore not stained. The gates in panel B in Figure G.2 was set according to the isotype control which resulted in approximately 100% of the population staining negative for all the stains. From these results, the set gate was concluded to be appropriate to use to determine troponin T expression of WT and Het KO iPSCs.

Appendix H: ICC results for negative control for characterization of iPSC-CMs

In this appendix, the results for the negative control for characterization of iPSC-CMs by ICC is presented. The negative control was only stained with Hoechst stain and secondary antibodies, without any primary antibodies. The result is visualized in Figure H.1.

Figure H.1. Negative control for characterization of iPSC-CMs by ICC. From left to right, the Hoechst stain is visualized in blue, Alexa Fluor 647 Goat anti-Mouse in cyan and Alexa Fluor 568 Goat anti-Rabbit in magenta. The scalebar measures 100 µm.

As seen in Figure H.1. the secondary antibodies are not visualized in the absence of primary antibodies which confirms that the iPSC-CMs are not autofluorescent.